Biobased dynamic hydrogels by reversible imine bonding for controlled release of thymopentin

Rui Yu, Eddy Petit, Mihail Barboiu, Suming Li, Wenjing Sun, Congmei Chen

Materials Science & Engineering C

Biobased dynamic hydrogels by reversible imine bonding for controlled release of thymopentin

--Manuscript Draft--

Manuscript Number:	MSEC-D-21-01195R1
Article Type:	Research Paper
Keywords:	O-carboxymethyl chitosan; Imine bonding; Dynamic hydrogel; Thymopentin; drug release; Density functional theory
Corresponding Author:	Suming Li University of Montpellier Montpellier, France
First Author:	Suming Li
Order of Authors:	Suming Li
	Rui Yu
	Eddy Petit
	Mihail Barboiu
	Wenjing Sun
	Congmei Chen
Abstract:	Thymopentin (TP5) is widely used in the treatment of autoimmune diseases, but the short in vivo half-life of TP5 strongly restricts its clinical applications. A series of blank and TP5 loaded hydrogels were synthesized via reversible dual imine bonding by mixing water soluble O-carboxymethyl chitosan (CMCS) with a dynamer (Dy) prepared from Jeffamine and benzene-1,3,5-tricarbaldehyde. TP5 release from hydrogels was studied at 37°C under in vitro conditions. The molar mass of CMCS, drug loading conditions and drug content were varied to elucidate their effects on hydrogel properties and drug release behaviors. Density functional theory was applied to theoretically confirm the chemical connections between TP5 or CMCS with Dy. All hydrogels exhibited interpenetrating porous architecture with average pore size from 59 to 83 μm, and pH-sensitive swelling up to 10 000 % at pH 8. TP5 encapsulation affected the rheological properties of hydrogels as TP5 was partially attached to the network via imine bonding. Higher TP5 loading led to higher release rates. Faster release was observed at pH 5.5 than at pH 7.4 due to lower stability of imine bonds in acidic media. Fitting of release data using Higuchi model showed that initial TP5 release was essentially diffusion controlled. All these findings proved that the dynamic hydrogels are promising carriers for controlled delivery of hydrophilic drugs, and shed new light on the design of drug release systems by both physical mixing and reversible covalent bonding.
Suggested Reviewers:	thierry Delair thierry.delair@univ-lyon1.fr
	elmira arab-tehrany elmira.arab-tehrany@univ-lorraine.fr
	katarzyna jelonek kjelonek@cmpw-pan.edu.pl
Response to Reviewers:	Dear editor and reviewers, Many thanks to the reviewers for their pertinent comments. We revised our manuscript accordingly and highlighted in red the changes in the revision. A point-to-point reply is given. We hope the paper is now acceptable for publication. Thanks. Sincerely yours, Suming LI

Re: Manuscript Number: MSEC-D-21-01195

Dear editor,
Many thanks to the reviewers for their pertinent comments. We revised our manuscript accordingly and highlighted in red the changes in the revision. A point-to-point reply is given below.
We hope the paper is now acceptable for publication. Thanks.
Sincerely yours,
Suming LI

Responses to the comments of Referee 1

This manuscript reported the preparation of the dynamic hydrogel by reversible imine bond crosslinking for sustained release of thymopentin. The mechanism is also confirmed by density functional theory. Therefore, I recommend its publication, but some revisions should be addressed before publication:

Comment 1: "The Abstract is not attractive and tedious, which looks like the conclusion. Please revise it."

Response: Thanks for this comment. The whole abstract is revised accordingly and marked in red.

Comment 2: "The mechanical properties of hydrogels should be supplied such as tensile strength and modulus et al. In addition, the optical photograph should also be presented."

Response: We agree with the reviewer that mechanical properties such as the tensile strength and modulus are important parameters of hydrogels. In the case of our dynamic hydrogels, they are "soft" hydrogels and used as carriers for in vitro drug release. As shown in Fig. 3, the storage modulus (G′) varies from hundreds to 2300 Pa, and is stable in the studied strain/frequency range. Moreover, TP5-loaded hydrogels maintained their structural integrity after drug release for 7 days. Therefore, rheological analysis can elucidate the feasibility of these dynamic hydrogels in drug release. Currently, we're focusing on obtaining better malleability of hydrogels for applications as wound dressing, and related tensile strength and modulus measurements will be conducted.
The as prepared hydrogels are transparent, and the optical photograph has been shown in a previous paper [1].

Comment 3: "Is the drug uniformly distributed in the hydrogel? How could you prove that?"

Response: Thymopentin is a highly hydrophilic drug [2, 3], and its saturation concentration in water is above 100 mg/mL. For all cases of TP5-loaded hydrogels in this manuscript (0.1 mg/ ml, 3 mg/ ml, 9 mg/ ml), the TP5 concentration is much lower than its saturation concentration. Moreover, TP5-loaded hydrogels were synthesized by in-situ encapsulation method. In other words, TP5 was homogeneously dissolved in the mixed aqueous solution of CMCS-Dynamer, and then gelation proceeded at 37 ℃. Therefore, it can be assumed that TP5 is uniformly

distributed in the hydrogel volume.

Comment 4: "Please supply the drug loading capacity of hydrogels."
Response: As mentioned in the Section 2.5 of the manuscript, in situ incorporation of TP5 results in complete drug encapsulation. Therefore, the drug loading capacity of TP5-loaded hydrogels is 100 %. Moreover, before in vitro release, all the TP5-loaded hydrogels were washed 3 times using PBS (pH 7.4), and the washing PBS solution was collected and analysed by HPLC-UV. No TP5 was detected, confirming that the TP5 was completely embedded in the hydrogel volume.
According to the reviewer's comment, the following phrase is added at the end of Section 2.5 (Page 7) : "In situ incorporation of TP5 results in complete drug encapsulation. Therefore, the drug loading capacity of all the TP5-loaded hydrogels is 100 %.".

References

[1] R. Yu, Y. Zhang, M. Barboiu, M. Maumus, D. Noël, C. Jorgensen, S. Li, Carbohydr. Polym., 244 (2020) 116471.

[2] Y. Yin, D. Chen, M. Qiao, Z. Lu, H. Hu, J. Controlled Release, 116 (2006) 337-345.

[3] Y. Xu, G. Li, W. Zhuang, H. Yu, Y. Hu, Y. Wang, Journal of Materials Chemistry B, 6 (2018) 7495-7502.

Responses to the comments of Referee 2

Authors prepared interesting biobased reversible imine hydrogels based on carboxymethyl chitosan, Jeffamine and benzene-1,3.5-tricarbaldehyde. The produced hydrogels are interesting but it is not clear how the presented system differs from the earlier work of the authors presented in ref 31-33. Is it only the application to TP5 loading and release? Authors should more clearly present the advancement to state of the art and novelty of the current work in relation to the previous works. Otherwise the work is relatively well-presented and organized and could be revised according to following points.
Response:
Thanks for the reviewer's pertinent comment. Similar hydrogels have been reported in our previous papers. This work focuses on the design of novel drug delivery systems by both physical mixing and reversible covalent bonding. Moreover, the effect of the molar mass of CMCS on the hydrogel properties and drug release behaviors is studied.
According to the reviewer's comment, the following phrase is added: "CMCS with different molar masses of CMCS was used since the molar mass affects the physico-chemical properties of hydrogels.".

Comment 1: "Introduction could be improved to better provide the background and important

state of the art and finally the hypothesis and novelty definition for the current work. Now the different paragraph feels separate and the "story" is not clear and fluent."
Response: Revision is made to better present the background and the state of the art (Pages 3, 4, 5). Two new references were cited (ref. 15, ref. 35).
The hypothesis and novelty of the manuscript were added in the last paragraph, Introduction part, according to the reviewer's comment.

Comment 2: "Page 5, 2.2: How was the concentration of remaining aldehyde groups measured?"
Response: As shown in note b) of Table 1: The concentration of Dy solution was obtained from the remaining aldehyde groups. In a typical reaction, 0.5 mmol BTA (81 mg) reacted with 0.5 mmol Jeffamine ED2003 (950 mg) to form a Dy solution. As BTA had 3 aldehydes and Jeffamine 2 amines, there remained theoretically 0.5 mmol of aldehydes in the dried Dy. Addition of 10 mL water yielded a dynamer solution of 0.05 M.

Comment 3: "Fig 1: The FT-IR evidence of TP5 incorporation in the hydrogels is very weak. The incorporation should be shown and quantified also by other means."
Response: We agree with the reviewer that the characteristic band at 1512 cm^{-1} is rather weak for Gel80K-TP5. Nevertheless, this band is significant. As shown in Fig.1 a-b), Gel80K-TP5, Dy-TP5, and TP5 present this characteristic band at 1512 cm^{-1} which is assigned to the N-H pending of amines in TP5. This band was not observed for the other samples, including Gel80K, Dy, and CMCS. This confirms the incorporation of TP5 in the hydrogel. Noticeably, the N-H band is weak because it is adjacent to the intense carbonyl groups band at 1595 cm^{-1}. Moreover, as shown in Fig. 2, NMR was another efficient means to verify the imine bonding between TP5 and the Dynamer, thus indirectly evidence the attachment of TP5 in the hydrogel network. Compared with the spectrum of Dy, no signals in the range of 10.1-10.2 ppm were observed on the spectrum of Dy-TP5, implying that all the remaining aldehydes of Dy had reacted with the amine groups of TP5, in agreement with FTIR data (Fig. 1b).

Comment 4: "The chemical structure of the hydrogels should be better confirmed and characterized. Now only one small FT-IR spectrum is presented for Gel80K"
Response: As mentioned in Section 2.2, 2.4 and 2.5 in the manuscript, the hydrogel frameworks were crosslinked via dual imine bonding from CMCS, Jeffaimine and BTA with well known structures. Therefore, FT-IR analysis is an efficient means for the characterization of samples by comparison of characteristic bands such as aldehyde, amine, and imine bands, as reported in our previous papers (ref. 33, 34 in manuscript).

Comment 5: "Fig 2. the NMR spectra. The chemical structures of the compounds or important chemical bonds should be drawn and the most important signals assigned in the NMR spectra."
Response: The chemical structures of all the compounds are shown in Scheme 1. Thus, they are not drawn in Fig. 2 as there is no space. Fig. 2 is largely modified. And in particular, assignment of all the signals of TP5 is given. Changes are made in Page 14 and Page 15.

Comment 6: "It would be interesting to add the pore diameter and especially to porosity of the

hydrogels."

Response: According to the reviewer's comment, the pore size distributions of as-prepared blank hydrogels are added in Fig. 4 and related discussion is added in Page 18 and Page 19.

Comment 7: "The mass loss ratios of the hydrogels is huge. How crosslinked are they, it seems crosslinking degree is very small? The original gel content of the hydrogels should be determined by extraction with suitable solvent."

Response: It's true that the mass loss ratio is high, especially in acidic medium due to the lower stability of imine bonds at low pH. In media around physiological pH, lower mass loss ratios are obtained. In the case of Gel80K, the mass loss ratio is only 30 % at pH 7.

As shown in Scheme 1, hydrogels are crosslinked by dual imine bonding in two steps: first between the aldehydes of BTA and the amines of Jeffamine (4 h at 70°C in methanol) to yield a dynamer, and then between the remaining aldehydes of BTA and the amines of CMCS (24 h at 37°C in water). As shown in Table 1, the concentrations of CMCS and Dy in hydrogels are 1.8 and 4.3 w/v%, respectively. It's probable that part of Dy is not involved in the hydrogel network, and is washed away during swelling, thus leading to relatively high mass loss as reported in our previous paper (ref. 33 in manuscript).

Concerning the determination of the original gel content of the hydrogels, the suitable solvent is water. This the original gel content can be considered as the remaining gel content after swelling 24 h at pH 7.4 because of the rapid swelling and mass loss (as shown in Fig. S4). According to the mass loss ratio after 24 h (Fig. 5b), the original gel contents are 64.5 % for Gel80K, 44.3% for Gel30K, and 46.5 % for Gel25K.

Comment 8: "The drug release rate is quite fast originally and also large amount of drug is not finally released. Is this really suitable for real applications?"

Response: We agree with the reviewer that in the first stage, the release rate is relatively fast. However, as described in the manuscript, TP5 was in-situ loaded in hydrogels via chemical and physical linkages, and TP5 release can be tuned by varying many parameters (e.g., drug load content, drug loading condition, pH of release medium, etc.). Although the burst release is fast, hydrogels can keep sustainable release up to 7 days. Thus, TP5 release would be further improved in the following work.

High unreleased amount of TP5 was obtained only for low loading concentration (0.1 and 3 mg/mL). When increasing the loading concentration to 9 mg/mL, the unreleased ratio decreases to 10 %. Therefore, by adjusting the loading condition, the unreleased rate can be tuned. On the other hand, TP5 release rate in pH 5.5 is much faster than that in pH 7.4 due to the fact that the imine bond is prone to hydrolyse in acidic condition (Fig. 7b). This would be very interesting for tumour therapy because of the slightly acidic pH in tumour. Therefore, these dynamic hydrogels crosslinked by dual imine bonding could be promising in cancer therapy by local administration.

- *O*-carboxymethyl chitosan-based dynamic hydrogels are synthesized by dual-imine bonding
- Thymopentin-loaded dynamic hydrogels are fabricated by *in-situ* encapsulation
- As-prepared hydrogels exhibit strongly pH-sensitive swelling behaviors
- *In vitro* release of thymopentin can be tuned by varying parameters, including pH of the release medium, drug load, and hydrogel preparation
- Density functional theory theoretically confirms the chemical connections between thymopentin and hydrogel network

Graphical Abstract

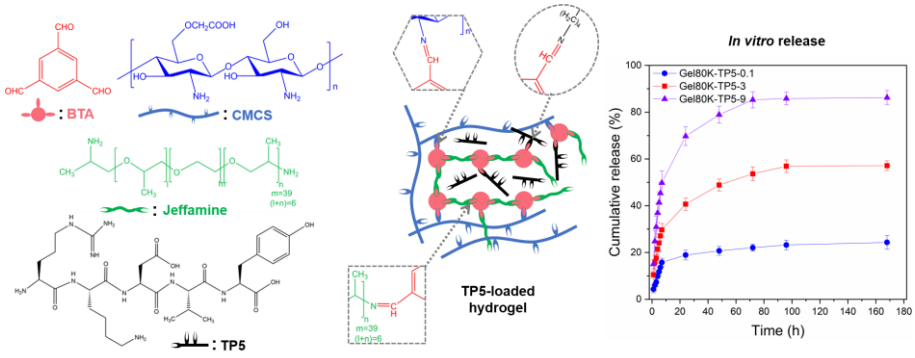

Thymopentin was loaded in O-carboxymethyl chitosan-based hydrogels via physical mixing and imine bonding. *In vitro* release was investigated, and analyzed using Higuchi model and density functional theory computation.

Declaration of interest statement

On behalf of all co-authors, I wish to confirm that there are no conflicts of interest associated with this publication untitled “Biobased dynamic hydrogels by reversible imine bonding for controlled release of thymopentin”, and there has been no significant financial support for this work that could have influenced its outcome.

Sincerely,

Suming LI

Author statement

Rui Yu did the experiments and wrote the manuscript. Eddy Petit did the HPLC analyses. Mihail Barboiu participated in the design of the research. Suming Li conceived and supervised the research work, and revised the manuscript. Wenjing Sun conceived the Density functional theory (DFT) computation and wrote this part. Congmei Chen performed the the DFT computation.

Biobased dynamic hydrogels by reversible imine bonding for controlled release of thymopentin

Rui Yu,[1] Eddy Petit,[1] Mihail Barboiu,[1*] Suming Li,[1*] Wenjing Sun,[2*] Congmei Chen[3]

[1] *Institut Européen des Membranes, IEM, UMR 5635, Univ Montpellier, CNRS, ENSCM, Montpellier, France*

[2] *China-America Cancer Research Institute, Key Laboratory for Medical Molecular Diagnostics of Guangdong Province, Guangdong Medical University, Dongguan, Guangdong 523808, China.*

[3] *National Supercomputing Center in Shenzhen (Shenzhen Cloud Computing Center), Guangdong, Shenzhen, 518055, China*

* Corresponding authors: suming.li@umontpellier.fr (S. Li); mihail-dumitru.barboiu@umontpellier.fr (M. Barboiu); swj_gdmc@163.com (W. Sun)

Abstract

Thymopentin (TP5) is widely used in the treatment of autoimmune diseases, but the short *in vivo* half-life of TP5 strongly restricts its clinical applications. A series of blank and TP5 loaded hydrogels were synthesized via reversible dual imine bonding by mixing water soluble *O*-carboxymethyl chitosan (CMCS) with a dynamer (Dy) prepared from Jeffamine and benzene-1,3,5-tricarbaldehyde. TP5 release from hydrogels was studied at 37°C under in vitro conditions. The molar mass of CMCS, drug loading conditions and drug content were varied to elucidate their effects on hydrogel properties and drug release behaviors. Density functional theory was applied to theoretically confirm the chemical connections between TP5 or CMCS with Dy. All hydrogels exhibited interpenetrating porous architecture with average pore size from 59 to 83 μm, and pH-sensitive swelling up to 10 000 % at pH 8. TP5 encapsulation affected the rheological properties of hydrogels as TP5 was partially attached to the network via imine bonding. Higher TP5 loading led to higher release rates. Faster release was observed at pH 5.5 than at pH 7.4 due to lower stability of imine bonds in acidic media. Fitting of release data using Higuchi model showed that initial TP5 release was essentially diffusion controlled. All these findings proved that the dynamic hydrogels are promising carriers for controlled delivery of hydrophilic drugs, and shed new light on the design of drug release systems by both physical mixing and reversible covalent bonding.

Keywords: *O*-carboxymethyl chitosan; Imine bonding; Dynamic hydrogel; Thymopentin; Drug release; Density functional theory

1. Introduction

Thymopentin (TP5) is a synthetic pentapeptide (Arg-Lys-Asp-Val-Tyr, M_n = 679.77) associated with the residual sequence (32-36) of thymic hormone thymopoietin [1, 2]. It possesses the biological properties characteristic of thymopoietin [3], and has been widely used for immunomodulation [4], and for treatments of autoimmune diseases [5], including cancer immunodeficiency [6], rheumatoid arthritis [7], tuberculosis [8], chronic heart failure [9], and chronic lymphocytic leukemia [10]. TP5 can facilitate the differentiation of thymocytes and affect the function to induce maturation of T-cells [11, 12] and bone marrow dendritic cells [13]. Nevertheless, due to the short half-life ($\leq$ 30 s in plasma) and extensive metabolism in the gastrointestinal tract [14], TP5 is generally applied as a freeze-dried powder by intramuscular or percutaneous injection [5]. Chronic autoimmune diseases require long therapies and repetitive injections of TP5 which could provoke complications. These disadvantages highly limit the clinical utilization of TP5.

It has been reported that the in vivo efficiency of TP5 can be improved by slow infusion [15]. Therefore, controlled drug delivery systems are considered as an appealing strategy to achieve slow infusion of TP5, including nanoparticles [16], micelles [17], liposomes [18], and hydrogels [19, 20]. These various systems present many advantages such as prolonged drug release, constant drug concentration, reduced side effects, protection of drugs from degradation, etc. Micelles, liposomes and nanoparticles have been used to encapsulate TP5, but the encapsulation efficiency is quite low because of its high hydrophilicity [17, 21]. Dissolving microneedle array was studied as a new strategy for TP5 delivery by transdermal injection [4]. However, customized microneedle arrays and daily administration are needed, leading to high cost and low bioavailability. In contrast, hydrogel delivery systems appear most interesting for sustained delivery of hydrophilic drugs, and have been used clinically [22]. Hydrogels can easily encapsulate a variety of hydrophilic therapeutic agents, including small-molecule drugs [23], macromolecular drugs [24] and cells [25]. Furthermore, the high-water up taking capacity endows hydrogels with the physical features similar to tissues, and excellent biocompatibility. Besides, the crosslinked framework of hydrogels can hinder penetration of proteins [26], and thus protecting vulnerable bioactive drugs from degradation by inwardly diffusing enzymes [27].

Hydrogels have been investigated for the encapsulation of TP5. Zhang et al. developed

a physical hydrogel from polylactide-poly(ethylene glycol) (PLA-PEG) block copolymers via stereo-complexation between poly(L-lactide) and poly(D-lactide) blocks [19]. High drug loading and rapid drug release were obtained. Nevertheless, PLA degradation leads to acidic by-products which could provoke inflammatory reactions, and such physical hydrogels exhibit low stability and mechanical strength. Su et al. synthesized a hydrogel by crosslinking PLA grafted *O*-carboxymethyl chitosan (CMCS) using 1-(3-dimethylaminopropyl)-3-ethylcarbodiimide (EDC) and *N*-hydroxysuccinimide (NHS) as crosslinking agents [28]. The resulting hydrogel was used to encapsulate TP5 by immersion of dried gel in a TP5 solution. More than 80% of TP5 was released in 48 h. However, the presence of residual chemicals or solvents could compromise the biocompatibility of the system [29]. Therefore, it becomes a major challenge to develop a delivery system of TP5 which exhibits good biocompatibility, stability and high encapsulation efficiency.

CMCS is a water-soluble derivative of chitosan, the second most abundant polysaccharide in nature. It has been studied as a promising carrier for the delivery of peptides and proteins [30]. On the other hand, Jeffamine is a biocompatible polyetheramine containing poly(propylene oxide) (PPO) and poly(ethylene oxide) (PEO) blocks, as well as primary amino groups at chain ends. It has been used in drug delivery because of its water solubility and cytocompatibility [31]. Recently, our group has developed a CMCS and Jeffamine based dynamic hydrogel that could be potentially used for drug delivery [32], cartilage engineering [33], and antibacterial materials [34]. The hydrogel was prepared via dual imine bond crosslinking between the amino groups of CMCS and the aldehyde ones of a 3D dynamer (Dy). Dy was first obtained by Schiff-base reaction of 1,3,5-benzenetrialdehyde (BTA) and di-amino Jeffamine, followed by Schiff-base reaction of Dy and CMCS in aqueous solution to yield a 3D network. Trifunctional BTA served as a core to ensure 3D crosslinking, and Jeffamine as a linker to endow Dy with aqueous solubility. The gelation process is conducted in aqueous solution under mild conditions, which is beneficial for encapsulation of fragile drugs

such as proteins or peptides [22]. Different from other chitosan-based hydrogel by imine bonding [35], CMCS and Jeffamine based dynamic hydrogels exhibit regular and interconnected porosity which is beneficial for swelling, diffusion of physiological fluids, and drug encapsulation [33,34]. Interestingly, the hydrogel network contains free aldehyde and amino groups which are able to react with the functional groups of drugs or other bioactive molecules.

This work aimed to develop a novel delivery system of TP5 from CMCS and Jeffamine based dynamic hydrogels by in situ encapsulation. CMCS with different molar masses of CMCS was used since the molar mass affects the physico-chemical properties of hydrogels. *In situ* incorporation of TP5 within the dynamic hydrogel should allow to achieve complete drug encapsulation by physical adhesion to pore walls and reversible imine bonding to the hydrogel network via Schiff base reaction between the amino groups of TP5 and aldehydes of the dynamer. The rheological properties, internal morphology and swelling performance of dynamic hydrogels and TP5-loaded hydrogels were comparatively investigated. *In vitro* drug release of TP5-loaded hydrogels was studied under different conditions, and fitted using Higuchi's model. Finally, density functional theory (DFT) was applied to model the different imine bonds in the hydrogel network.

2. Experimental section

2.1 Materials

O,*O*'-bis(2-aminopropyl) poly(propylene glycol)-block-poly(ethylene glycol)-block-poly(propylene glycol), namely Jeffamine® ED-2003 with M_n of 1900, methanol (96%), hydrogen peroxide solution (H_2O_2, 30%) citric acid (99.5%), disodium hydrogen phosphate dodecahydrate (99%), boric acid (99.5 %), and borax (99%) were all of analytical grade, and obtained from Sigma-Aldrich. Benzene-1,3,5-tricarbaldehyde (BTA, purity 98%) was purchased from Manchester Organics. *O*-carboxymethyl chitosan (CMCS) with degree of carboxymethylation of 80 %, degree of deacetylation of 90 % was supplied by Golden-shell Biochemical Co., Ltd. TP5 (99%) was purchased from Soho-Yiming Pharmaceutical Co., LTD (Shanghai, China). All chemicals were

used as received without further purification.

2.2 Synthesis of dynamer

A dynamer (Dy) was synthesized from Jeffamine and BTA, as reported in our previous work [33]. Typically, BTA (81 mg, 0.5 mmol) and Jeffamine (0.95 g, 0.5 mmol) were dissolved in 20 mL methanol. The mixture was then heated to 70 °C and allowed to react for 4 h under gentle stirring. The solvent was totally removed by using rotary evaporator. 10 mL Milli Q water was added to yield a homogeneous Dy solution at a concentration of 0.05 M, as calculated from the remaining aldehyde groups.

2.3 Depolymerization of CMCS

Low molar mass CMCS was prepared via degradation of original CMCS in the presence of H_2O_2 [36]. Typically, CMCS (1 g) was dissolved in 30 mL Milli-Q water under stirring at 25 ℃. 0.15 mL H_2O_2 was then dropped in the solution. After 30 min degradation, the solution was immediately freezed by immersing in liquid nitrogen, and transferred onto a freeze dryer. After 24 h lyophilization, a white powder was obtained. The product was dissolved in 10 mL Milli-Q water, followed by precipitation in 200 mL absolute ethanol. Finally, the product was obtained by vacuum drying at 40℃ for 24 h. Another product was obtained after 60 min degradation using the same process. The M_n of original CMCS and depolymerized ones for 30 and 60 min are 80 000, 30 000 and 25 000, respectively, as determined by GPC in aqueous medium. They are accordingly named as CMCS80K, CMCS30K and CMCS25K.

2.4 Preparation of dynamic hydrogels

Dynamic hydrogels were prepared from CMCS, Jeffamine and BTA as previously reported [33, 34]. Typically, CMCS solution (0.15 M) was prepared by dissolving 0.318 g CMCS (1.5 mmol, calculated from D-glucosamine units) in 10 mL Milli-Q water at room temperature. The CMCS solution (0.15 M) was then mixed with the Dy solution

(0.05 M) with a 4/1 molar ratio of glucosamine/Dy. After removal of trapped bubbles by using ultra-sound, gelation was allowed to proceed at 37 ℃ for 24 h to yield a transparent hydrogel named as Gel80K, Gel30K or Gel25K according to the M_n of CMCS.

2.5 Preparation of TP5 loaded hydrogels

TP5 loaded hydrogels were prepared through *in situ* encapsulation. In brief, 2.625 mg TP5 was dissolved in 0.5 mL CMCS80K (0.15 M). The resulting solution was mixed with 0.375 mL Dy solution (0.05 M). The glucosamine of CMCS to Dy molar ratio was 4/1. After removal of bubbles, gelation then proceeded at 37 ℃ for 24 h to yield a TP5-loaded hydrogel with TP5 concentration of 3 mg/mL, namely Gel80K-TP5-3. Other TP5 loaded hydrogels were prepared using the same procedure but changing one parameter: Gel80K-TP5-0.1, Gel80K-TP5-9, Gel80K-TP5-3 (25°C) whose gelation occurred at 25°C, and Gel80K-TP5-3B prepared by dissolving TP5 in Dy solution before mixing with CMCS80K solution. TP5 was also loaded in Gel30K or Gel25K, and the corresponding samples were named as Gel30K-TP5-3 or Gel25K-TP5-3, respectively. In situ incorporation of TP5 results in complete drug encapsulation. Therefore, the drug loading capacity of all the TP5-loaded hydrogels is 100 %.

2.6 Characterization

^{1}H NMR spectroscopy was carried out using Bruker NMR spectrometer (400-LS) at 400 MHz. D_2O was used as the solvent. 5 mg of sample were dissolved in 0.5 mL of solvent for each analysis.

Gel permeation chromatography (GPC) was performed on a Water 1515 multidetector GPC system equipped with Waters 410 differential detector and ultra-hydrogel 250 column. 0.1 M NaCl was used as the mobile phase with a flow velocity of 0.6 mL/min. The column temperature was set at 40 ℃, and the sample concentration was 5.0 mg/mL. Poly(ethylene glycol) standards were used for calibration.

Fourier-transform infrared (FT-IR) spectroscopy of freeze-dried hydrogels was conducted on Nicolet Nexus FT-IR spectrometer, equipped with ATR diamant Golden Gate.

The morphology of freeze-dried hydrogels was examined by using Hitachi S4800 scanning electron microscopy (SEM). As-prepared hydrogels were placed in small vials, and immersed in liquid nitrogen (-196 °C) in order to conserve the original structure. The frozen samples were lyophilized with LABCONCO® freeze dryer for 24 h, and sputter coated prior to analysis.

Physical MCR 301 Rheometer (Anton Paar) was utilized to determine the rheological properties of hydrogels, using a cone plate geometry (diameter of 4 cm, apex angle of 2°, and clearance of 56 μm). The storage modulus (G′) and loss modulus (G″) were measured as a function of time, strain or frequency.

2.7 Swelling of freeze-dried hydrogels

The swelling performance of freeze-dried gels was evaluated by immersion in buffer solutions at different pH values. Buffers from pH 3 to pH 7.4 were prepared from 0.1 M citric acid and 0.2 M disodium hydrogen phosphate dodecahydrate solutions, buffers at pH 8 and pH 9 from 0.2 M boric acid and 0.05 M borax solutions, and buffer at pH 10 from 0.05 M borax and 0.2 M sodium hydroxide solutions. Freeze-dried gel samples were immersed in a buffer solution, and taken out after 24 h. The swollen hydrogels were weighed after wiping surface water with filter paper, and weighed again after 24 h lyophilization. The swelling and mass loss ratios of hydrogels were calculated according to the following equations:

$$\text{Swelling ratio } \% = \frac{(M_s - M_d)}{M_d} \times 100 \quad \text{(Eq. 1)}$$

$$\text{Mass loss ratio } \% = \frac{(M_0 - M_d)}{M_0} \times 100 \quad \text{(Eq. 2)}$$

Where M_0 is the initial mass of dried gel, M_s is the wet mass of the swollen hydrogel, and M_d is the dried mass of the swollen hydrogel after lyophilization.

2.8 *In vitro* release of TP5

In vitro drug release was realized in pH = 7.4 phosphate buffered saline (PBS) at 37 ℃. TP5-loaded hydrogel samples were placed in a centrifuge tube (50 mL) containing 10 mL pH 7.4 PBS. *In vitro* release was performed in shaking water bath at 37 ℃. At preset time intervals, 3 mL of the buffer solution were taken out, and replaced by 3 mL fresh buffer. TP5 concentration of the release supernatant was determined by HPLC-UV. A calibration curve was previously established using TP5 solutions with known concentrations. *In vitro* release of TP5 was also conducted in acidic buffer (pH 5.5), using the same procedure.

The cumulative release of TP5 was calculated using equation 3:

$$Release\ rate = \frac{V_e \sum_1^{n-1} C_i + V_0 C_n}{M_{drug}} \times 100 \quad \text{(Eq. 3)}$$

Where C_n and C_i represent the drug concentrations in the supernatant for n and i withdrawing steps, respectively; V_0 is initial total volume of PBS; V_e is collected volume of PBS; M_{drug} is the original loading amount of TP5. The drug loading efficiency is 100 % due to the *in situ* encapsulation of TP5. All of the experiments were performed in triplicate, and values were given in mean ± SD for n = 3.

2.9 The release kinetics model

The release kinetics of the various TP5-loaded hydrogel systems were studied by fitting the *in vitro* release data using Higuchi's model [37, 38]:

$$Q_t = K_H \times t^{\frac{1}{2}} \quad \text{(Eq. 4)}$$

where Q_t is the quantity of drug released within the time t, K_H is the Higuchi dissolution constant.

2.10 Density functional theory (DFT) computation

All calculations were performed using the Dmol^3 code in the Materials Studio 7.0 package [39]. The GGA/PBE functional was selected, and double numerical plus polarization (DNP) was used as the basis set [40]. Convergence tolerances for the total

energy, maximum force, and maximum displacement were set to 1.0×10^{-5} Hartree, 2.0×10^{-3} Hartree/Å, and 5.0×10^{-3} Hartree/Å, respectively. The self-consistent field convergence was 1.0×10^{-6} Hartree. To accelerate the self-consistent field (SCF) convergence, the smearing was set to 0.005 Hartree. The solvent effect was simulated by conductor-like screening model (COSMO) [41], using the dielectric constant of 78.54 (water). The transition states were calculated by using the synchronous method with conjugated gradient refinements. This method involves linear synchronous transit (LST) maximization, followed by repeated conjugated gradient (CG) minimizations, then quadratic synchronous transit (QST) maximizations and repeated CG minimizations until a transition state is located [42]. The energy barrier ($E_{Barrier}$) was calculated using equation 5:

$$E_{Barrier} = E_{TS} - E_{IN} \quad \text{(Eq. 5)}$$

where E_{TS} is the energy of the transition state, and E_{IN} the energy of the intermediate connected to the transition state.

The reaction energy (E_{RE}) of the elementary steps was calculated using equation 6:

$$E_{RE} = E_P - E_R \quad \text{(Eq. 6)}$$

where E_P is the energy of the elementary reaction product, and E_R the initial energy of the elementary reaction reactant.

3. Results and discussion

3.1 Preparation of hydrogels

Dynamic hydrogels were synthesized via Schiff-base reaction between CMCS and the dynamer, as shown in Scheme 1. Upon mixing CMCS and Dy aqueous solutions, the amino groups along the CMCS backbone react with the remaining aldehyde groups of Dy, resulting in formation of a 3D hydrogel network by dual imine bonding. The CMCS to Dy molar ratio of 4:1 was adopted since it allows optimal crosslinking, as demonstrated in our previous work [33]. In situ TP5 encapsulation in hydrogels is also shown in Scheme 1. Table 1 summarizes all the details for the preparation of blank and

drug loaded hydrogels.

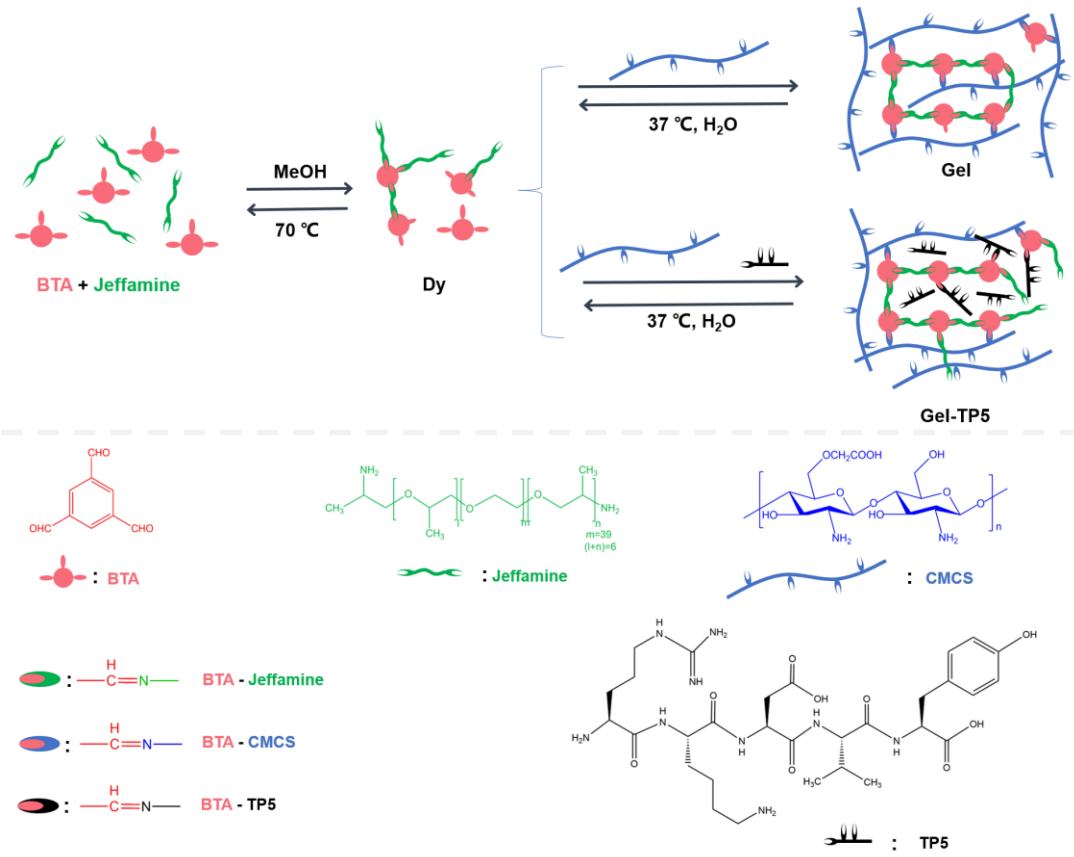

Scheme 1. Synthesis of dynamic hydrogels via Schiff-base reaction between CMCS and Dy, and in-situ loading of TP5 in hydrogels.

Table 1. Molar and mass compositions of blank and TP5 loaded hydrogels [a)]

Sample	CMCS80K		CMCS30K		CMCS25K		Dy [c)]		TP5 [f)]
	[mmol] [b)]	[w/v%]	[mmol] [b)]	[w/v%]	[mmol] [b)]	[w/v%]	[mmol]	[w/v%]	[mg/mL]
Gel80K	0.3	1.8	-	-	-	-	0.075	4.3	-
Gel30K	-	-	0.3	1.8	-	-	0.075	4.3	-
Gel25K	-	-	-	-	0.3	1.8	0.075	4.3	-
Gel80K-TP5-0.1	0.3	1.8	-	-	-	-	0.075	4.3	0.1

Gel80K-TP5-3	0.3	1.8	-	-	-	-	0.075	4.3	3
Gel80K-TP5-3B [d]	0.3	1.8	-	-	-	-	0.075	4.3	3
Gel80K-TP5-3 (25 ℃) [e]	0.3	1.8	-	-	-	-	0.075	4.3	3
Gel80K-TP5-9	0.3	1.8	-	-	-	-	0.075	4.3	9
Gel30K-TP5-3	-	-	0.3	1.8	-	-	0.075	4.3	3
Gel25K-TP5-3	-	-	-	-	0.3	1.8-	0.075	4.3	3

a) Hydrogels were prepared by mixing the aqueous solutions of 0.15 M CMCS80K/CMCS30K/CMCS25K and 0.05 M Dy at a D-glucosamine/Dy molar ratio of 4/1 (total volume of 3.5 mL), TP5 loaded hydrogels were prepared by adding TP5 in CMCS solution before mixing with Dy solution; b) Moles of glucosamine units of CMCS. Calculations were made on the basis of the average molar mass of 212 g/mol obtained for D-glucosamine, taking into account the degree of deacetylation of 90% and the degree of carboxymethylation of 80%; c) The concentration of Dy solution was obtained from the remaining aldehyde groups. In a typical reaction, 0.5 mmol BTA (81 mg) reacted with 0.5 mmol Jeffamine ED2003 (950 mg) to form a Dy solution. As BTA had 3 aldehydes and Jeffamine 2 amines, there remained theoretically 0.5 mmol of aldehydes in the dried Dy. Addition of 10 mL water yielded a dynamer solution of 0.05 M. d) Gel80K-TP5-3B was prepared by adding TP5 in Dy solution before mixing with CMCS solution e) Gel80K-TP5-3 (25 ℃) was prepared at 25 ℃; f) The concentration of TP5 in hydrogel was 0.1 mg/ml or 3 mg/ml or 9 mg/ml.

3.2 FT-IR and NMR

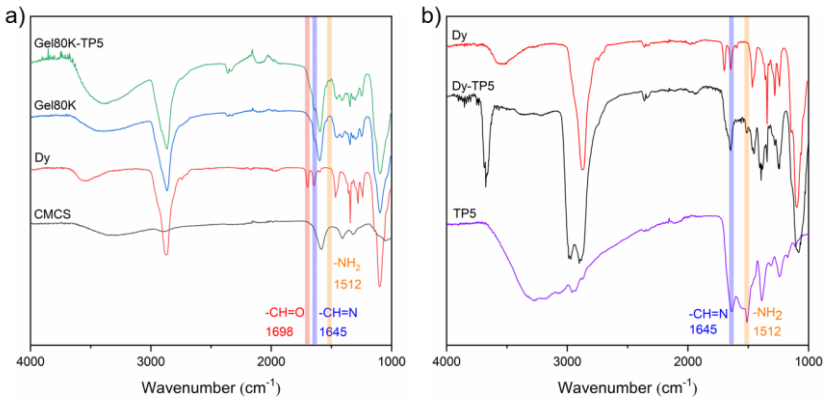

Fig. 1. a) FT-IR spectra of freeze-dried CMCS, Dy, Gel80K and Gel80K-TP5-3; b) FT-IR spectra of Dy, TP5, and Dy-TP5 which is an obtained by mixing TP5 in Dy solution at a molar ratio of 1/1, reaction at 37℃ for 24h, and 24 h lyophilization.

Fig. 1a shows the FTIR spectra of CMCS, Dy, freeze dried Gel80K and TP5 loaded

Gel80K-TP5-3. CMCS presents a large band around 3350 cm^{-1} which is attributed to free OH and NH_2 groups, and an intense band at 1595 cm^{-1} due to carbonyl groups. The dynamer exhibits two intense bands at 2850 and 1100 cm^{-1} assigned to C-H and C-O stretching, and two characteristic bands at 1698 and 1645 cm^{-1} corresponding to aldehyde and imine bonds, respectively. All the characteristic bands of CMCS and Dy are observed on the spectrum of freeze dried Gel80K. Nevertheless, the band of aldehyde groups at 1698 cm^{-1} is almost invisible, but the band at 1645 cm^{-1} corresponding to newly formed imine bonds is clearly distinguished. These results illustrate that hydrogels are formed due to imine formation between aldehydes of Dy and amine groups of CMCS. On the spectrum of Gel80K-TP5-3, a band is detected at 2100 cm^{-1}, which is assigned to the O-H stretching of water [43]. In fact, the freeze-dried samples rapidly absorbed water due to the high hygroscopicity of TP5 [44, 45]. Similar findings are obtained for other blank and TP5 loaded hydrogels (Fig. S1).

Fig. 1b presents the FT-IR spectra of Dy, TP5 and a Dy-TP5 mixture. The latter was prepared in order to figure out the reactions between the aldehydes of Dy and the amines of TP5. It was obtained by dissolving TP5 in Dy solution at a molar ratio of 1/1, followed by 24 h reaction at 37 ℃ and finally 24 h lyophilization. TP5 presents characteristic bands at 1630 and 1512 cm^{-1} which are assigned to the C=O stretching of amides and N-H pending of amines, together with a large band around 3300 cm^{-1} due to the presence of water. Interestingly, the band of aldehydes at 1698 cm^{-1} is not detected on the spectrum of Dy-TP5, suggesting that the aldehydes have reacted with the amine groups of TP5 via Schiff-base reaction.

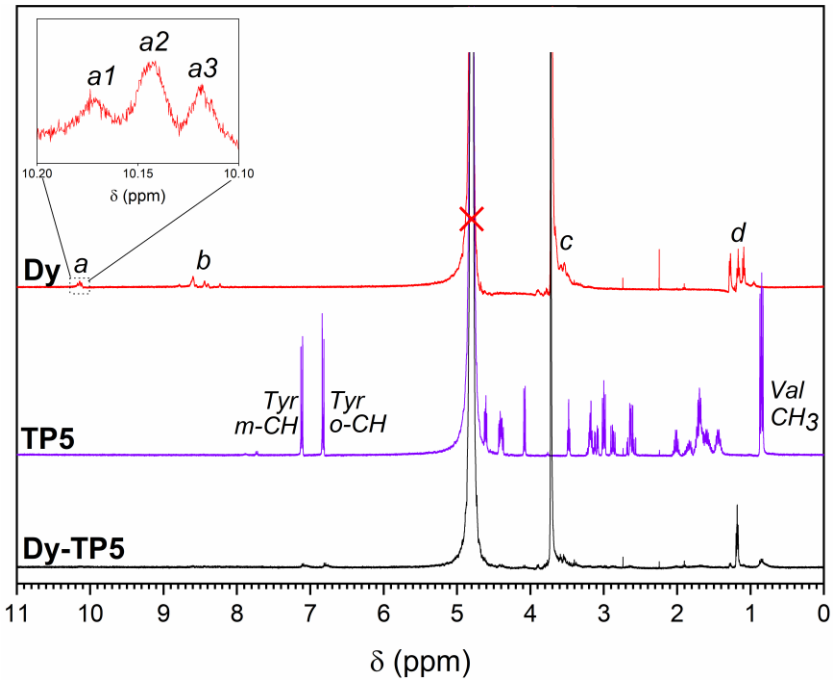

Fig. 2. ^{1}H NMR spectra of the Dy, TP5, and Dy-TP5 in D_2O.

Fig. 2 shows the ^{1}H NMR spectra of the Dy, TP5, and Dy-TP5. On the spectrum of Dy, the three small signals in the 10.1-10.2 ppm range are assigned to aldehyde groups of BTA with different degrees of substitution, including non-substituted (a1), mono-substituted (a2), and di-substituted aldehydes (a3). Signals between 8.2 and 8.7 ppm belong to the aromatic protons of BTA and imine protons (b). Signals around 3.7 ppm are assigned to the methylene and methine protons (c) of Jeffamine, and signals between 1.0 and 1.3 ppm to the methyl protons (d) of Jeffamine [33, 34]. The presence of residual H_2O is detected at 4.8 ppm. TP5 presents numerous signals associated to the various protons of the pentapeptide (Arg-Lys-Asp-Val-Tyr). The two doublets around 7.15 and 6.85 ppm are assigned to the meta-CH (Tyr m-CH) and ortho-CH (Tyr o-CH) on the phenyl ring of tyrosine [46], respectively. The three signals between 4.0 and 4.7 ppm belong to the various methine protons, and the signals between 1.3 and 3.6 ppm to the various methylene protons of the pentapeptide. The strong signal at 0.85 ppm is attributed to the methyl protons of valine (Val CH_3) [46]. Importantly, no signals in the range of 10.1-10.2 ppm are observed on the spectrum of Dy-TP5, implying that all the remaining aldehydes of Dy have completely reacted with the amine groups of TP5, in

agreement with FTIR data (Fig. 1b).

The morphology of CMCS, Dy, their mixtures with TP5 (CMCS-TP5 and Dy-TP5) was examined by using SEM (Fig. S2). No obvious difference is observed between pristine CMCS (Fig. S2a, b) and CMCS-TP5 (Fig. S2e, f). Both samples display a lamellar structure with the presence of holes of *c.a* 10 µm, suggesting the absence of interactions between the two components. In contrast, difference is detected between pristine Dy (Fig. S2c, d) and the mixture Dy-TP5 (Fig. S2g, h). Both samples exhibit a highly porous structure. The surface of Dy appears rugged, whereas that of Dy-TP5 appears smooth. These findings seem to indicate the occurrence of interactions between TP5 and the Dy.

3.3 Rheology

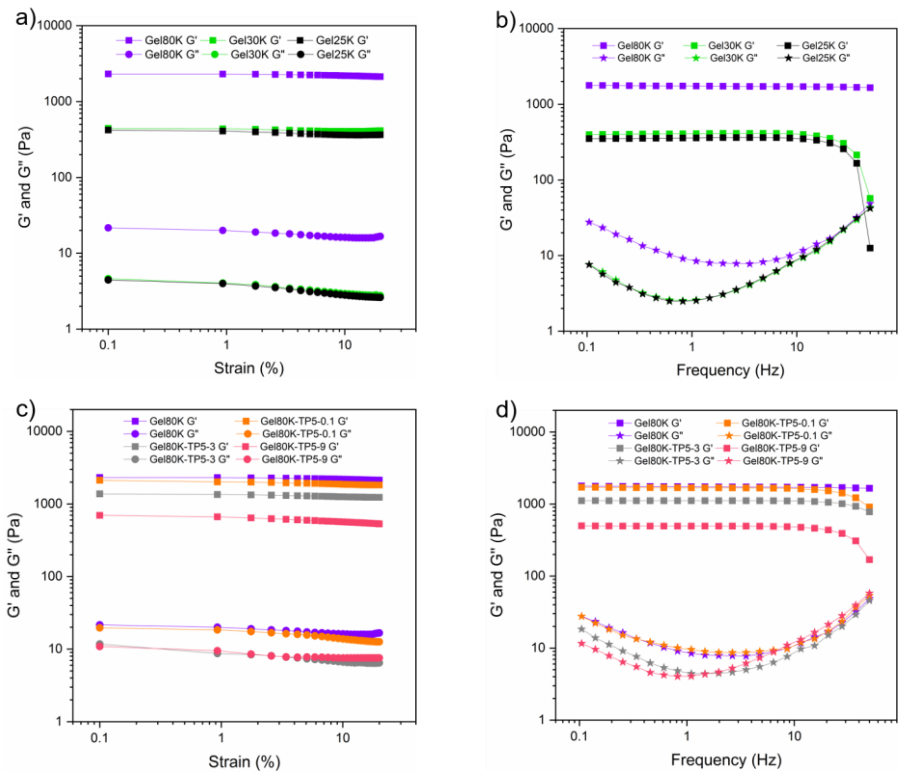

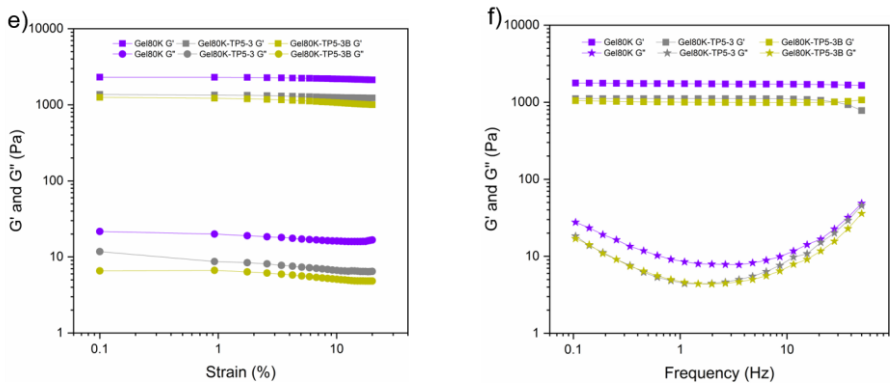

Fig. 3. Storage modulus (G′) and loss modulus (G″) changes of Gel80K, Gel30K and Gel25K as a function of strain at 25 °C and at 1 Hz (**a)** and as a function of frequency at 25 °C and at a strain of 1 % (**b)**; G′ and G″ changes of Gel80K, , Gel80K-TP5-0.1, Gel80K-TP5-3 and Gel80K-TP5-9 as a function of strain at 25 °C and at 1 Hz (**c)** and as a function of frequency at 25 °C and at a strain of 1% (**d)**; G′ and G″ changes of Gel80K, Gel80K-TP5-3, and Gel80K-TP5-3B as a function of strain at 25 °C and at 1 Hz (**e)** and as a function of frequency at 25 °C and at a strain of 1 % (**f)**.

Rheological measurements were conducted on the various hydrogels at 25 °C to evidence the effect of CMCS molar mass on the rheological properties as well as the interaction between TP5 and Dy in the hydrogel network. Firstly, the storage modulus (G′) and loss modulus (G″) changes of blank hydrogels (Gel80K, Gel30K and Gel25K) were determined as a function of strain at a frequency of 1 Hz and at 25 °C, as shown in Fig. 3a. As the strain increases from 0.1 % to 20 %, G′ remains almost constant for all the blank hydrogels, whereas G″ slightly decreases, indicating a linear viscoelastic (LVE) behavior of hydrogels in the 0.1 to 20 % strain range. Meanwhile, the moduli of blank hydrogels are highly dependent on the molar mass of CMCS. With the decrease of molar mass of CMCS from 80,000 to 30,000 and to 25,000, G′ at a strain of 1% decreases from 2300 Pa for Gel80K to 440 Pa for Gel30K, and to 420 Pa for Gel25K, respectively. Similar phenomena are observed for G″ changes. In fact, higher molar mass chains have more amino groups, which allows to enhance the crosslinking density, thus resulting in higher modulus of hydrogels

Fig. 3b shows the modulus changes of blank hydrogels as a function of frequency from 0.1 Hz to 50 Hz at a constant strain (1%) and at 25 °C. G′ remains constant in the whole frequency range for Gel80K, whereas a sharp decrease of G′ is observed beyond 30 Hz in the cases of Gel30K and Gel25K. On the other hand, G″ exhibits some fluctuations with increasing frequency. These rheological results well corroborate with the formation of highly stable covalent networks, in contrast to physical hydrogels whose storage and loss moduli increase with increasing frequency due to chain entanglements [19, 47]. It is also noteworthy that Gel80K exhibit higher stability than Gel30K and Gel25K due to higher crosslinking density as mentioned above.

Fig. 3c presents G′ and G″ changes *versus* strain of Gel80K hydrogels containing various amounts of TP5 (0, 0.1, 3, and 9 mg/mL). Obviously, with addition of TP5 in hydrogels, G′ decreases from 2310 Pa for Gel80K to 2222 Pa for Gel80K-TP5-0.1, to 1374 Pa for Gel80K-TP5-3, and to 697 Pa for Gel80K-TP5-9. These results illustrate that *in situ* TP5 encapsulation affects the rheological properties of drug loaded hydrogels. In fact, the amine groups of TP5 can react with the free aldehyde groups of Dy, as shown in Fig. 1b and Fig. 2. Hence, there is competition between TP5 and CMCS after mixing aqueous solution of Dy with that of CMCS and TP5, leading to decreased imine bonding between CMCS and Dy. On the other hand, attachment of TP5 to the network does not contribute to the crosslinking because TP5 is a small molecule compared to CMCS. Therefore, the crosslinking density decreases with increase of TP5 content, and consequently the modulus of hydrogels decreases. A frequency sweep of hydrogels was performed over a range from 0.01 to 50 Hz at a fixed strain of 1 %. G′ remains constant for Gel80K, and slightly decreases beyond 30 Hz for TP5 loaded hydrogels, indicating that TP5 encapsulation affects the stability of hydrogels.

A hydrogel (Gel80K-TP5-3B) was prepared by dissolving TP5 in Dy solution, followed by mixing with CMCS solution before gelation. As TP5 is supposed to react with Dy, dissolving TP5 in Dy solution should favor imine formation between them. G′ and G″ changes of Gel80K, Gel80K-TP5-3, and Gel80K-TP5-3B were examined as a

function of strain and frequency (Fig. 3e, f). Noticeably, G′ of Gel80K-TP5-3 is higher than that of Gel80K-TP5-3B in nearly the whole strain and frequency ranges, which confirms that mixing TP5 and Dy first decreased the crosslinking density of hydrogels. Strain and frequency sweeps were also performed on blank and TP5 loaded Gel30K and Gel25K hydrogels (Fig. S3). Similar phenomena were observed, illustrating the stability of hydrogels and interactions between TP5 and the dynamer.

3.4 Morphology and swelling properties

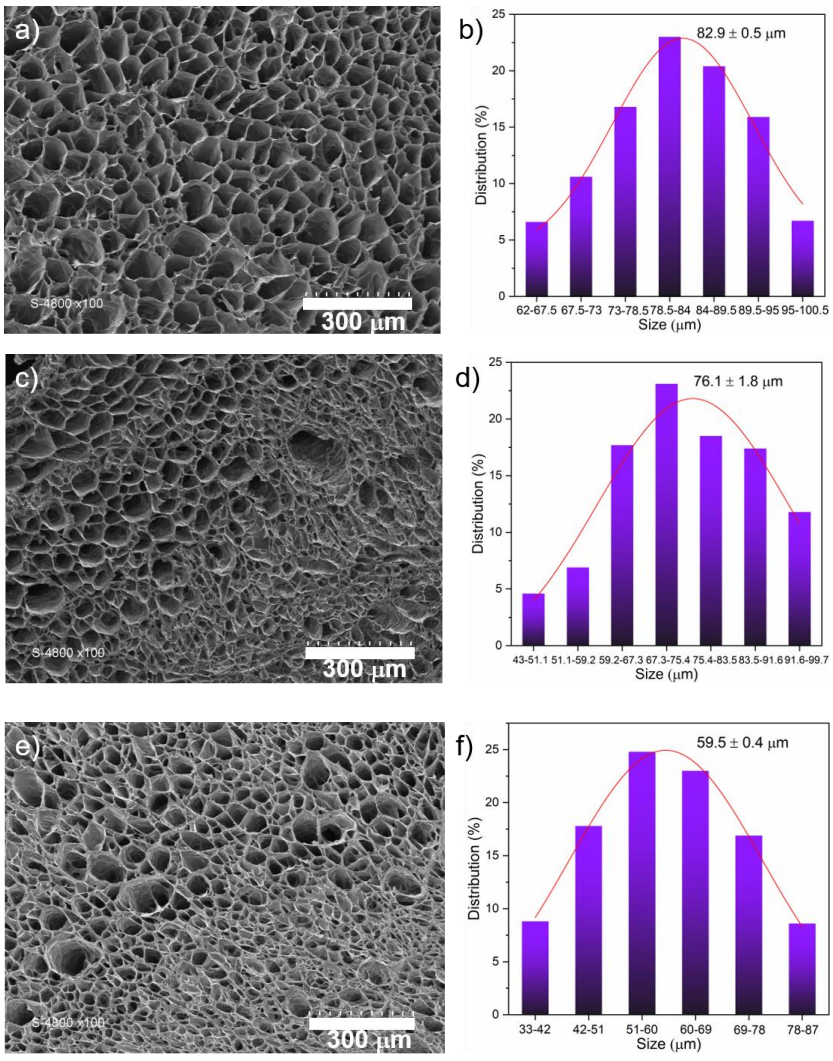

Fig. 4. SEM images and pore size distributions of freeze-dried gels: (a, b) Gel80K; (c, d) Gel30K; (e, f) Gel25K.

The morphology of as-prepared hydrogels after lyophilization was observed by SEM. Obviously, all hydrogels exhibit interpenetrating and porous architectures. Compared to Gel30K and Gel25K, Gel80K displays more regular structure and narrower distribution of interconnected pores (Fig. 4a). The average pore diameter of Gel80K, Gel30K and Gel25K is 82.9 ± 0.5 μm (Fig. 4b), 76.1 ± 1.8 μm (Fig. 4d), and 59.5 ± 0.4 μm (Fig. 4f), respectively. Thus, it seems that the pore diameter slightly decreases with decrease of the molar mass of CMCS. Moreover, in a previous work, it was shown that the pore diameter of dynamic hydrogels is dependent on the molar mass of Jeffamine linker [34]. Therefore, the porous structure of dynamic hydrogels can be tailored by varying the molar mass of the components. On the other hand, the interconnected porous structure enables hydrogels to mimic the extracellular matrix, which is beneficial for biomedical applications in drug delivery [48], and in tissue engineering [33, 49]. Therefore, Gel80K which has the optimal porous "spongy" characteristics was selected as the carrier of an in-depth study of drug release.

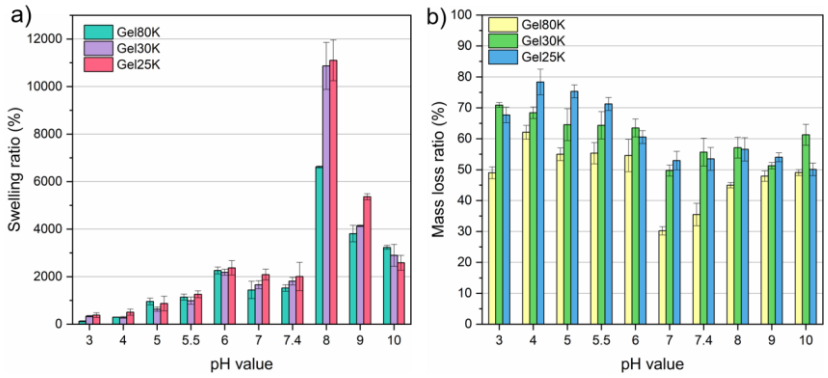

Fig. 5. a) Swelling ratios, and b) Mass loss ratios of Gel80K, Gel30K and Gel25K after 24 h immersion in buffers at various pH values. Data are expressed as mean ± SD for n = 3.

As aforementioned, the most important characteristic of hydrogels is their capability to retain large amount of water in the polymeric network, which is beneficial for controlling the release profiles of drugs and the absorption of wound exudate [50]. Fig. 5a presents the swelling performance of freeze-dried hydrogels in buffers at various pH

values. All the hydrogels exhibit a highly pH-dependent swelling behavior. The swelling degree is relatively low (< 1000 %) in strong acid buffers (pH 3/4), and increases to around 2000 % from pH 4 to 6. It remains at the same level around 2000 % in the pH 6 to 7.4 range. All hydrogels exhibit a maximum swelling at pH 8, 6600 % for Gel80K, 10000 % for Gel30K, and 11000 % for Gel25K. As the alkalinity continues to increase to pH 9 and 10, the swelling degree of hydrogel deceases dramatically to a level around 3000 %. In addition, there is no major difference between the swelling ratios of the three samples except at pH 8. The pH sensitivity of the swelling of hydrogels is assigned to electrostatic interactions between the amino and carboxyl groups along CMCS chains [33, 51]. In fact, the pK_a of amino and carboxyl groups of CMCS is 6.5 and 2.7, respectively. Contraction of hydrogels occurs because of strong electrostatic attraction between negatively charged $-COO^-$ and positively charged $-NH_3^+$ groups which result from protonation in strong acidic media (pH 3 and 4), thus leading to low swelling ratio. Electrostatic attraction diminishes with the decrease of the H^+ concentration (pH 5, 5.5, and 6), and thus the swelling gradually increases. At pH 6, 7 and 7.4 which are around the pK_a of amino groups, the swelling remains almost constant as the electrostatic interactions are weak due to low concentrations of charges. In contrast, high swelling of hydrogels occurs because of strong repulsion between negatively charged $-COO^-$ groups at pH 8. Nevertheless, with higher alkalinity at pH 9 and 10, OH^- ions in solution would counterbalance the electrostatic repulsion between $-COO^-$ groups [33], thus resulting in decrease of the swelling degree. The pH sensitive swelling of hydrogels could be of great importance for the design of drug delivery systems due to large variation of physiological pH at various body sites in normal and pathological conditions [52].

Mass loss of hydrogels occurs during the swelling process due to the solubilization and washing away of non-crosslinked species, as shown in Fig. 5b. Overall, the mass loss ratio of all the hydrogels varies between 30 % and 80 % in the whole pH range. The hydrogels show higher mass loss in acid conditions than in neutral and alkaline

conditions. Noticeably, the mass loss ratio of Gel80K is lower than those of Gel30K and Gel25K in the whole pH range. This finding could be attributed to the better cross-linking Gel80K as compared to Gel30K and Gel25K because Gel80K was prepared from CMCS80K with higher molar mass, in agreement with rheological data. The lowest mass loss ratio is 30 and 36 % obtained for Gel80K at pH 7 and 7.4, respectively, in agreement with the better stability of Gel80K at neutral pH. Thus, Gel80K is used for a comprehensive study of TP5 release from hydrogels under various conditions.

The swelling and mass loss behaviors of Gel80K were investigated under drug release conditions in pH 7.4 PBS at 37 ℃ up to 168 h (Fig. S4, Information supplementary). The swelling ratio rapidly increases to 750 % and 1200 % after immersion for 10 and 20 min, respectively, whereas the mass loss ratio increases 25 % and 32 % in the meantime. Thereafter, the swelling and mass loss ratios remain almost at the same level up to 168 h, fluctuating around 1300 % and 34 %, respectively. These findings indicate that an equilibrium is rapidly reached after immersion of dried gels in PBS, and that the hydrogels are stable after initial mass loss.

3.5 *In vitro* release of the TP5

TP5 is an immuno-modulating drug, and is widely applied in the treatment of autoimmune diseases such as chronic lymphocytic leukemia [10], Sezary's syndrome [53, 54], etc. Besides, TP-5 is able to induce the differentiation of T-cells and accelerate the development of T lymphocytes [11]. A series of TP5-loaded hydrogels were prepared, including Gel80K-TP5-0.1, Gel80K-TP5-3, Gel80K-TP5-9, Gel80K-TP5-3B, Gel80K-TP5-3(25°C), Gel30K-TP5-3, and Gel25K-TP5-3 so as to evaluate the effects of various factors.

The morphology of the various TP5-loaded hydrogels was examined by using SEM (Fig. S5). It appears that TP5 encapsulation affects the regularity of the porous structure of hydrogels. In fact, Gel80K-TP5-0.1 exhibits a porous structure similar to that of Gel80K (Fig. 4a,b), but the surface appears rougher. With increase of TP5 content from

0.1 mg/mL (Fig. S5a, b) to 3 mg/mL (Fig. S5c, d), and to 9 mg/mL (Fig. S5e, f), the three-dimensional architecture becomes more and more irregular as compared with that of Gel80K (Fig. 4a,b). Similarly, TP5 encapsulation also affects the structure of Gel30K-TP5-3 (Fig. S5i, j) and Gel25K-TP5-3 (Fig. S5k, l) as compared to corresponding blank hydrogels. On the other hand, difference is also noticed between the morphology of Gel80K-TP5-3 and Gel80K-TP5-3B (Fig. S5g, h). Both have exactly the same compositions, but different mixing orders. Gel80K-TP5-3B exhibits a smoother surface compared to Gel80K-TP5-3.

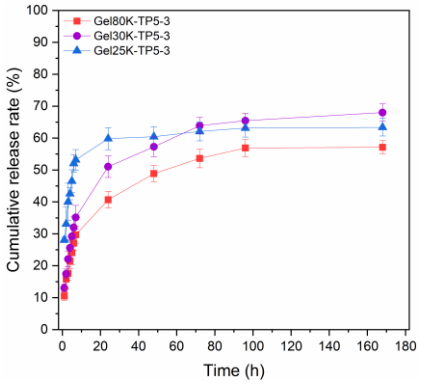

Fig. 6. Cumulative release of TP5 from Gel80K-TP5-3, Gel30K-TP5-3, and Gel25K-TP5-3. Values were expressed as mean ± SD for n = 3.

TP5 release from the various TP5-loaded hydrogels was monitored to evaluate the potential of dynamic hydrogels as drug carrier in cancer therapy [38]. Fig. 6 shows the release profiles of TP5 from Gel80K-TP5-3, Gel30K-TP5-3, and Gel25K-TP5-3 in pH 7.4 PBS at 37 ℃. Overall, all samples displayed a release profile in two stages, namely a burst release in the first 7 h followed by a slow and continuous release during 7 days. After 1 h in the medium, significant release rates are recorded, 28.0% for Gel25K-TP5, 13.0 % for Gel30K-TP5 and 10.5 % for Gel80K-TP5. TP5 release increases almost linearly to reach 53.2 %, 35.1 % and 29.7 % after 7 h for the 3 samples, respectively. Thereafter, TP5 release slows down, reaching a plateau after 96 h. The total TP5 release is 63.4, 68.0, and 57.1% after 168 h for Gel25K-TP5, Gel30K-TP5 and Gel80K-TP5, respectively. Gel80K-TP5 exhibits slower and more sustainable release as compared to

Gel25K-TP5 and Gel30K-TP5 due to its higher crosslinking density which disfavors drug diffusion. Therefore, Gel80K is used as drug carrier in further studies.

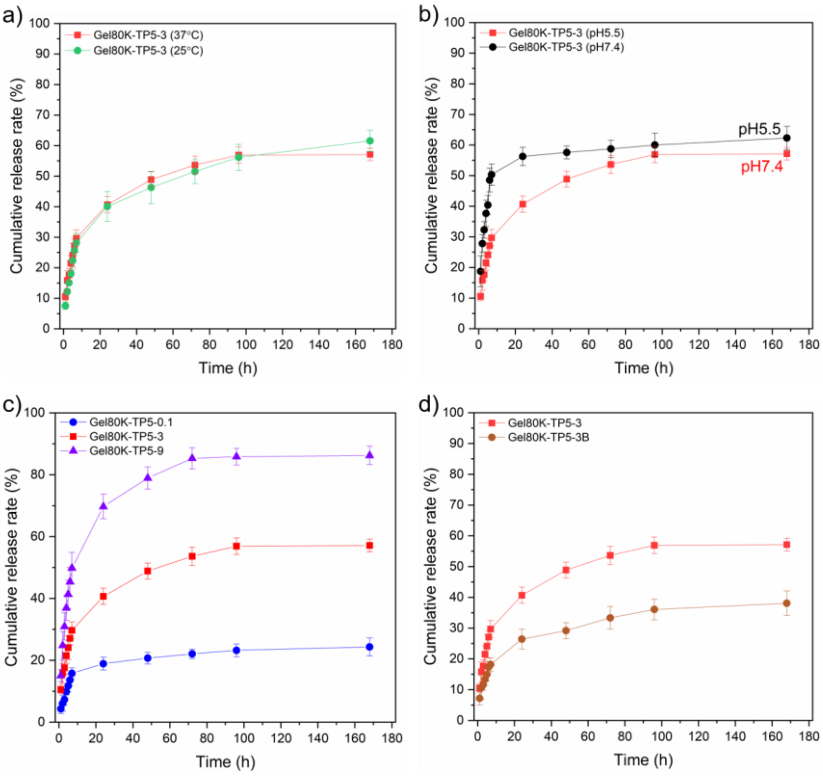

Fig. 7. a) Cumulative release of TP5 from Gel80K-TP5-3 prepared at 25 ℃ and 37 ℃, namely Gel80K-TP5-3 (25 ℃) and Gel80K-TP5-3 (37 ℃); b) Cumulative release of TP5 from Gel80K-TP5-3 in PBS at pH 7.4, and in acid buffer medium at pH 5.5, namely Gel80K-TP5-3 (pH 7.4) and Gel80K-TP5-3 (pH 5.5); c) Cumulative release of TP5 from Gel80K loaded with various TP5 contents: Gel80K-TP5-0.1, Gel80K-TP5-3, and Gel80K-TP5-9; d) Cumulative release of TP5 fromGel80K-TP5-3 and Gel80K-TP5-3B with different mixing orders. Values were expressed as mean ± SD for n = 3.

Fig. 7 show the TP5 release curves from various hydrogels. No difference is noticed between the release profiles Gel80K-TP5-3 prepared at 25 °C and at 37 °C (Fig. 7a), indicating the gelation temperature (25 or 37 °C) of Gel80K-TP5 has little impact on the release of TP5. In contrast, faster initial release is observed from Gel80K-TP5-3 at pH 5.5 than at pH 7.4, although both present similar equilibrium release ratios around

60% (Fig. 7b). This difference can be assigned to the fact that the imine bonds are prone to hydrolysis under acidic condition [55], which leads to partial disassociation of the three-dimensional hydrogel network thus favoring the diffusion of trapped TP5. It is also of interest to evaluate the effect of initial drug load on the release rate by comparing the release profiles of Gel80K-TP5-0.1, Gel80K-TP5-3, Gel80K-TP5-9, as shown in Fig. 7c. Apparently, the latter shows the highest equilibrium rate, reaching 90 % after 168 h, which is much higher than that of Gel80K-TP5-0.1 (22.5%) and Gel80K-TP5-3 (57 %). This difference well corroborates with the partial attachment of TP5 to the hydrogel network by imine bonding. It can be assumed that only free TP5 is released as imine bonds are stable at pH 7.4. Thus, hydrogels with higher drug loading have higher proportion of free drug, and consequently present higher drug release ratio [38]. Finally, TP5 release behaviors from Gel80K-TP5-3 and Gel80K-TP5-3B are compared to examine the effect of the mixing order (Fig. 7d). Gel80K-TP5-3B presents a total release ratio of 38%, which is much lower than that of Gel80K-TP5-3 (60%). This finding also confirms the covalent attachment of TP5 to the hydrogel network by imine bonding. As TP5 is first mixed with Dy before mixing with CMCS in the case of Gel80K-TP5-3B, more TP5 is covalently attached to the network, leading to lower TP5 release as compared to Gel80K-TP5-3. These data indicate that only physically encapsulated TP5 can be released under in vitro conditions. The release rate of TP5 from hydrogels depends on many factors such as the molar mass of CMCS, the pH of the medium, the drug load, and the mixing order during hydrogel preparation.

3.6 Drug release kinetics

Table 2 Parameters obtained from fitting of experimental data using Higuchi model [a)]

Sample	R^2	K_H
Gel80K-TP5-0.1	0.967	6.477
Gel80K-TP5-3	0.990	11.110
Gel80K-TP5-9	0.998	20.897

Gel80K-TP5-3B	0.978	6.502
Gel80K-TP5 (pH5.5)	0.982	19.141
Gel80K-TP5 (25℃)	0.985	12.271
Gel30K-TP5	0.997	13.315
Gel25K-TP5	0.986	16.172

a) Experimental data in Fig. 6-7.

It is widely admitted that the release of a hydrophilic drug from a monolithic matrix mainly depends on the diffusion process. Other factors such as physical forces between the drug and the hydrogel matrix and swelling of bulk hydrogel affect the release profile as well. Higuchi's model has been largely used to describe the drug release kinetics of various systems. It is based on the Fick's Law where the release proceeds by the diffusion of drugs through the delivery system. In this case, the cumulative released drug amount is proportional to the square root of time. TP5 release kinetics were investigated by fitting of experimental data in the first 6 h using Higuchi model in order to better understand the release mechanism of TP5 from dynamic hydrogels [38], as shown in Fig. S6 and Table 2.

Data in Table 2 show that the correlation coefficient is above 0.98 in all cases except Gel80K-TP5-0.1, suggesting that the TP5 release was mainly controlled by diffusion process [56]. In fact, the maximum concentration of TP5 after total release in the release medium is well below its saturation concentration (> 10 mg/mL) even for Gel80K-TP5-9 [19]. Thus, it could be considered that the dissolution is the ruling force of TP5 release from the hydrogels as drug release was conducted under immersion conditions [38]. It is also of interest to compare the K_H values of the different systems. Gel80K-TP5-9 and Gel80K-TP5-0.1 present the highest and the lowest K_H values, respectively, in agreement with the fastest and the slowest release rates. Intermediate K_H values were obtained for other TP5 loaded hydrogels.

3.7 Density functional theory (DFT) modelling

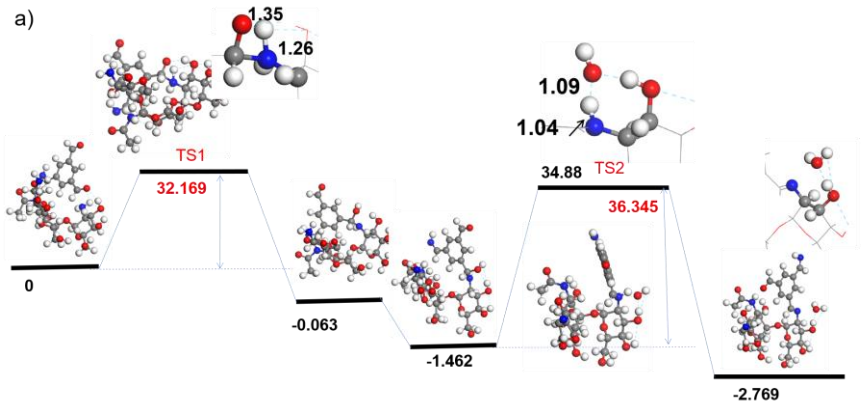
a)
1.35
1.26
TS1
32.169
0
-0.063
-1.462
1.09
1.04
34.88
TS2
36.345
-2.769

1

2

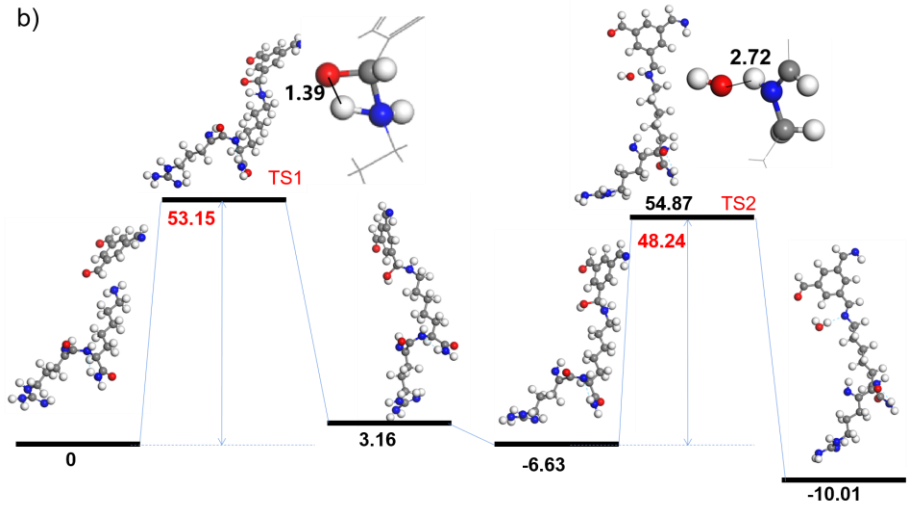
b)
1.39
TS1
53.15
0
3.16
2.72
54.87
TS2
48.24
-6.63
-10.01

3

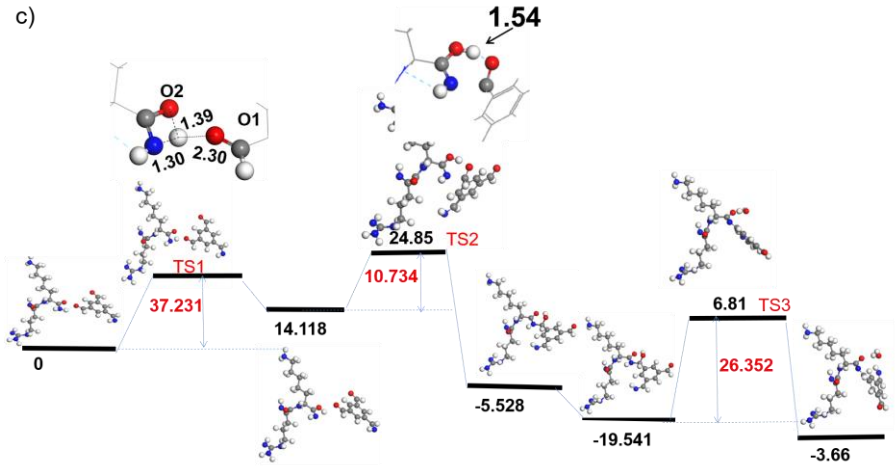
c)
1.54
O2
1.39
O1
1.30
2.30
TS1
37.231
0
14.118
24.85
TS2
10.734
-5.528
6.81
TS3
26.352
-19.541
-3.66

4

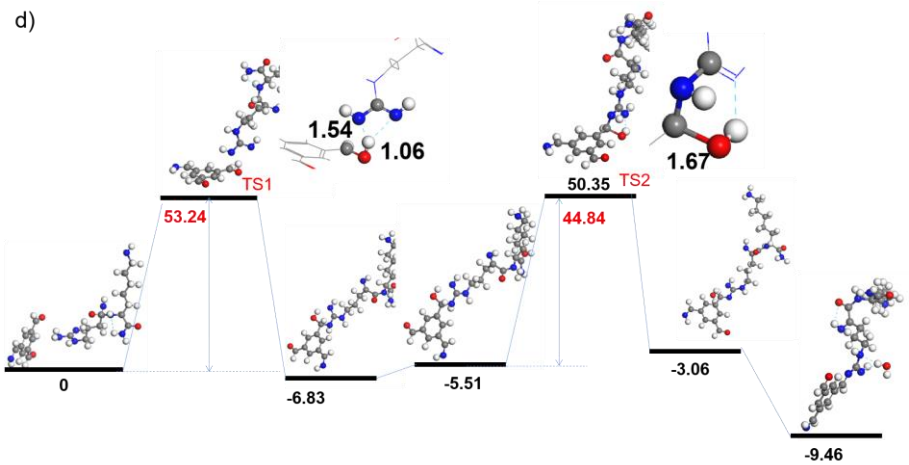

Fig. 8. Computation by density functional theory (DFT) to determine the lowest reaction pathways between : a) CMCS-l-Dy; b) TP5(1)-l-Dy (TP5 site 1); c) TP5(2)-l-Dy (TP5 site 2); and d) TP5(3)-l-Dy (TP5 site 3). The reaction energy and energy barrier are calculated by Eq. 5 and Eq. 6 in kcal/mol.

Density functional theory (DFT) was used to determine the reaction energy and energy barrier of imine linkages between TP5 and Dy (TP5-l-Dy, 'l' stands for linkage, similarly hereinafter) as well as those between CMCS and Dy (CMCS-l-Dy. The simplified models of CMCS, Dy and TP5 are shown in Fig. S7a-c. Only one reaction site is considered taking into account the repeatability of the amino groups in CMCS and the symmetry of Dy. The lowest energy pathway of the Schiff-base reaction between CMCS and Dy is shown in Fig. 8a. The first step of the reaction is the dehydrogenation from the amino group of Dy, which requires overcoming an energy barrier of 32.2 kcal/mol. The formation of CH-NH bond is thermodynamically favorable. This is followed by the cleavage of the oxhydryle group, which needs higher energy than the first step, reaching 36.3 kcal/mol. The formation and removing of H_2O molecule are thermodynamically favorable. Thus, the rate-limiting step of the reaction between CMCS and Dy is the cleavage of oxhydryle with an energy barrier of 36.3 kcal/mol.

There are three kinds of amino groups in TP5 which have different chemical environments (Fig. S7c). Thus, there are three -NH_2 sites that can be involved in the

Schiff-base reaction, which are marked as TP5(1)-l-Dy (Fig. 8b), TP5(2)-l-Dy (Fig. 8c) and TP5(3)-l-Dy (Fig. 8d), respectively. The Schiff-base reactions of TP5(1)-l-Dy and TP5(3)-l-Dy are similar. The rate-limiting step of both reactions is the dehydrogenation from the amino groups of TP5 (the first step), which needs to overcome an energy barrier of 53.15 and 53.24 kcal/mol, respectively. The reaction process to yield TP5(2)-l-Dy is more complex than those of the two other reactions. It begins with dehydrogenation from the amino group of TP5. But the H atom tends to bond with the adjacent oxygen atom (O2), and the process needs to overcome an energy barrier of 37.2 kcal/mol. In the second step, the hydrogen proton transfers from O2 to O1, which needs an energy of 10.7 kcal/mol. The formation of -C-NH bond is thermodynamically favorable. Subsequently, the cleavage of oxhydryle needs to overcome a barrier of 26.4 kcal/mol. Thus, the rate-limiting step of the reaction needs to overcome a barrier of 37.2 kcal/mol, which is only 0.9 kcal/mol higher than that of the Schiff-base reaction between CMCS and Dy. Thus, the -C=O group adjacent to the $-NH_2$ of TP5 could promote the Schiff-base reaction between TP5 and Dy to form TP5(2)-l-Dy. Moreover, the two other $-NH_2$ sites of TP5 may also participate in the Schiff-base reaction in spite of higher energy barrier. Hence, although the energy barrier of TP5-l-Dy is higher than that of CMCS-l-Dy, both reactions proceed concomitantly in a competitive way.

Furthermore, it is worth noting that the gelation time of blank hydrogel without TP5 is shorter than that of hydrogel containing TP5 (data not shown). Therefore, the presence of TP5 affects the crosslinking between CMCS and Dy because TP5 reacts competitively with Dy and formation of TP5-l-Dy does not contribute to the crosslinking due to steric effect. When TP5 is mixed with Dy, it can theoretically and experimentally react with Dy via Schiff base reaction, which is in full agreement with the results obtained by FT-IR (Fig. 1), NMR (Fig. 2), and SEM (Fig. S4), and TP5 release (Fig. 6 and 7).

4. Conclusion

This work focused on the synthesis and characterization of a novel drug delivery system based on dynamic hydrogels for the sustainable release of an immunostimulant – thymopentin (TP5). The hydrogels were prepared via *in situ* gelation of O-carboxymethyl chitosan with a dynamer made from Jefamine and BTA in aqueous solution by imine bonding, in the presence or absence of TP5. These hydrogels display a porous structure, outstanding rheological properties and excellent pH-sensitive swelling performance. Analyses showed that TP5 is partly attached to the hydrogel network by imine bonding, together with free TP5 molecules adsorbed by physical forces into the hydrogel pore walls. *In vitro* release showed a burst release in the first 24 h, followed by a slower release to reach a plateau up to 168 h. The maximum release rate depends on various factors such as drug content, drug loading and release conditions. Data show that only free TP5 is released under in vitro conditions. Covalently attached TP5 is not released due to the stability of imine bonds at pH 7.4. Density functional theory study allowed to better understand the chemical combination between the hydrogel's components and the drug. All these findings suggest that *in situ* gelation of water soluble CMCS with a 3D dynamer is a means of choice to design efficient release systems of hydrophilic drugs, in particular those containing amino groups which can be covalently attached to the hydrogel network. Last but not least, this study offers a simple and environmentally friendly strategy to prepare bioactive and biodegradable hydrogels for drug delivery systems.

Acknowledgement

This work is supported by the scholarship from China Scholarship Council (CSC), and the Institut Européen des Membranes (Exploratory project "Biostent - Health" of the Internal IEM Call 2017).

References

[1] G. Goldstein, T.K. Audhya, Thymopoietin to thymopentin: experimental studies, Surv. Immunol. Res., 4 (1985) 1, https://doi.org/10.1007/BF02919050.

[2] D.H. Schlesinger, G. Goldstein, The amino acid sequence of thymopoietin II, Cell, 5 (1975) 361-365, https://doi.org/10.1016/0092-8674(75)90054-9.
[3] G. Goldstein, M.P. Scheid, E.A. Boyse, D.H. Schlesinger, J. Van Wauwe, A synthetic pentapeptide with biological activity characteristic of the thymic hormone thymopoietin, Science, 204 (1979) 1309-1310, https://doi.org/10.1126/science.451537.
[4] S. Lin, B. Cai, G. Quan, T. Peng, G. Yao, C. Zhu, Q. Wu, H. Ran, X. Pan, C. Wu, Novel strategy for immunomodulation: Dissolving microneedle array encapsulating thymopentin fabricated by modified two-step molding technology, Eur. J. Pharm. Biopharm., 122 (2018) 104-112, https://doi.org/10.1016/j.ejpb.2017.10.011.
[5] T. Zhang, X. Qin, X. Cao, W. Li, T. Gong, Z. Zhang, Thymopentin-loaded phospholipid-based phase separation gel with long-lasting immunomodulatory effects: in vitro and in vivo studies, Acta Pharmacologica Sinica, 40 (2019) 514-521, https://doi.org/10.1038/s41401-018-0085-8.
[6] B. Bodey, B. Bodey Jr, S.E. Siegel, H.E. Kaiser, Review of thymic hormones in cancer diagnosis and treatment, Int. J. Immunopharmacol, 22 (2000) 261-273, https://doi.org/10.1016/S0192-0561(99)00084-3.
[7] B. Kantharia, N. Goulding, N. Hall, J. Davies, P. Maddison, P. Bacon, M. Farr, J. Wojtulewski, K. Englehart, S. Liyanage, Thymopentin (TP-5) in the treatment of rheumatoid arthritis, Rheumatology, 28 (1989) 118-123, https://doi.org/10.1093/rheumatology/28.2.118.
[8] Y. Wang, X. Ke, J.S. Khara, P. Bahety, S. Liu, S.V. Seow, Y. Yang, P.L.R. Ee, Synthetic modifications of the immunomodulating peptide thymopentin to confer anti-mycobacterial activity, Biomaterials, 35 (2014) 3102-3109, https://doi.org/10.1016/j.biomaterials.2013.12.049.
[9] X. Cao, Y. Li, Y. Guo, F. Cao, Thymopentin improves cardiac function in older patients with chronic heart failure, Anatolian journal of cardiology, 17 (2017) 24, https://doi.org/10.14744/AnatolJCardiol.2016.6692.
[10] R. Colle, T. Ceschia, A. Colatutto, F. Biffoni, Use of thymopentin in autoimmune hemolytic anemia due to chronic lymphocytic leukemia, Current therapeutic research, 44 (1988) 1045-1049.
[11] M. Zhu, W. Wan, H. Li, J. Wang, G. Chen, X. Ke, Thymopentin enhances the generation of T-cell lineage derived from human embryonic stem cells in vitro, Exp. Cell Res., 331 (2015) 387-398, https://doi.org/10.1016/j.yexcr.2014.12.012.
[12] M.S. Kondratyev, S.M. Lunin, A.V. Kabanov, A.A. Samchenko, V.M. Komarov, E.E. Fesenko, E.G. Novoselova, Structural and dynamic properties of thymopoietin mimetics, J. Biomol. Struct. Dyn., 32 (2014) 1793-1801, https://doi.org/10.1080/07391102.2013.834851.
[13] Y. Wang, Y. Cao, Y. Meng, Z. You, X. Liu, Z. Liu, The novel role of thymopentin in induction of maturation of bone marrow dendritic cells (BMDCs), Int. Immunopharmacol., 21 (2014) 255-260, https://doi.org/10.1016/j.intimp.2014.05.011.
[14] J.P. Tischio, J.E. Patrick, H.S. Weintraub, M. Chasin, G. Goldstein, Short in vitro half- life of thymopoietin 32–36 pentapeptide in human plasma, Int. J. Pept. Protein

Res., 14 (1979) 479-484, https://doi.org/10.1111/j.1399-3011.1979.tb01959.x.
[15] T. Audhya, G. Goldstein, Thymopentin (TP- 5) potency in vivo is enhanced by slow infusion, International journal of peptide protein research, 22 (1983) 568-572, https://doi.org/10.1111/j.1399-3011.1983.tb02130.x.
[16] X. Jin, Y. Xu, J. Shen, Q. Ping, Z. Su, W. You, Chitosan-glutathione conjugate-coated poly (butyl cyanoacrylate) nanoparticles: promising carriers for oral thymopentin delivery, Carbohydr. Polym., 86 (2011) 51-57, https://doi.org/10.1016/j.carbpol.2011.03.050.
[17] Y. Xu, G. Li, W. Zhuang, H. Yu, Y. Hu, Y. Wang, Micelles prepared from poly (N-isopropylacrylamide-co-tetraphenylethene acrylate)-b-poly [oligo (ethylene glycol) methacrylate] double hydrophilic block copolymer as hydrophilic drug carrier, Journal of Materials Chemistry B, 6 (2018) 7495-7502, https://doi.org/10.1039/C8TB02247J.
[18] J. Zuo, T. Gong, X. Sun, Y. Huang, Q. Peng, Z. Zhang, Multivesicular liposomes for the sustained release of thymopentin: stability, pharmacokinetics and pharmacodynamics, Die Pharmazie-An International Journal of Pharmaceutical Sciences, 67 (2012) 507-512, https://doi.org/10.1691/ph.2012.1126.
[19] Y. Zhang, X. Wu, Y. Han, F. Mo, Y. Duan, S. Li, Novel thymopentin release systems prepared from bioresorbable PLA–PEG–PLA hydrogels, Int. J. Pharm., 386 (2010) 15-22, https://doi.org/10.1016/j.ijpharm.2009.10.045.
[20] Y. Hu, Y. Liu, X. Qi, P. Liu, Z. Fan, S. Li, Novel bioresorbable hydrogels prepared from chitosan- graft- polylactide copolymers, Polym. Int., 61 (2012) 74-81, https://doi.org/10.1002/pi.3150.
[21] Y. Yin, D. Chen, M. Qiao, Z. Lu, H. Hu, Preparation and evaluation of lectin-conjugated PLGA nanoparticles for oral delivery of thymopentin, J. Controlled Release, 116 (2006) 337-345, https://doi.org/10.1016/j.jconrel.2006.09.015.
[22] J. Li, D. Mooney, Designing hydrogels for controlled drug delivery, Nature Reviews Materials, 1 (2016) 1-17, https://doi.org/10.1038/natrevmats.2016.71.
[23] J. Zhao, X. Zhao, B. Guo, P.X. Ma, Multifunctional interpenetrating polymer network hydrogels based on methacrylated alginate for the delivery of small molecule drugs and sustained release of protein, Biomacromolecules, 15 (2014) 3246-3252, https://doi.org/10.1021/bm5006257.
[24] S. Peers, A. Montembault, C. Ladavière, Chitosan hydrogels for sustained drug delivery, J. Controlled Release, 326 (2020) 150-163, https://doi.org/10.1016/j.jconrel.2020.06.012.
[25] X. Yang, G. Liu, L. Peng, J. Guo, L. Tao, J. Yuan, C. Chang, Y. Wei, L. Zhang, Highly efficient self- healable and dual responsive cellulose- based hydrogels for controlled release and 3D cell culture, Adv. Funct. Mater., 27 (2017) 1703174, https://doi.org/10.1002/adfm.201703174.
[26] J. Su, B. Hu, W.L. Lowe Jr, D.B. Kaufman, P.B. Messersmith, Anti-inflammatory peptide-functionalized hydrogels for insulin-secreting cell encapsulation, Biomaterials, 31 (2010) 308-314, https://doi.org/10.1016/j.biomaterials.2009.09.045.
[27] J.M. Reichert, Trends in development and approval times for new therapeutics in

the United States, Nature Reviews Drug Discovery, 2 (2003) 695-702, https://doi.org/10.1038/nrd1178.
[28] F. Su, J. Wang, S. Zhu, S. Liu, X. Yu, S. Li, Synthesis and characterization of novel carboxymethyl chitosan grafted polylactide hydrogels for controlled drug delivery, Polym. Adv. Technol., 26 (2015) 924-931, https://doi.org/10.1002/pat.3503.
[29] S.T.K. Raja, T. Prakash, A. Gnanamani, Redox responsive albumin autogenic nanoparticles for the delivery of cancer drugs, Colloids Surf. B. Biointerfaces, 152 (2017) 393-405, https://doi.org/10.1016/j.colsurfb.2017.01.044.
[30] Y. Lin, H. Liang, C. Chung, M. Chen, H. Sung, Physically crosslinked alginate/N, O-carboxymethyl chitosan hydrogels with calcium for oral delivery of protein drugs, Biomaterials, 26 (2005) 2105-2113, https://doi.org/10.1016/j.biomaterials.2004.06.011.
[31] A. Lu, E. Petit, S. Li, Y. Wang, F. Su, S. Monge, Novel thermo-responsive micelles prepared from amphiphilic hydroxypropyl methyl cellulose-block-JEFFAMINE copolymers, Int. J. Biol. Macromol., 135 (2019) 38-45, https://doi.org/10.1016/j.ijbiomac.2019.05.087.
[32] Y. Zhang, C. Pham, R. Yu, E. Petit, S. Li, M. Barboiu, Dynamic hydrogels based on double imine connections and application for delivery of fluorouracil, Frontiers in Chemistry, 8 (2020) 739, https://doi.org/10.3389/fchem.2020.00739.
[33] R. Yu, Y. Zhang, M. Barboiu, M. Maumus, D. Noël, C. Jorgensen, S. Li, Biobased pH-responsive and self-healing hydrogels prepared from *O*-carboxymethyl chitosan and a 3-dimensional dynamer as cartilage engineering scaffold, Carbohydr. Polym., 244 (2020) 116471, https://doi.org/10.1016/j.carbpol.2020.116471.
[34] R. Yu, L. Cornette de Saint-Cyr, L. Soussan, M. Barboiu, S. Li, Anti-bacterial dynamic hydrogels prepared from O-carboxymethyl chitosan by dual imine bond crosslinking for biomedical applications, Int. J. Biol. Macromol., 167 (2020) 1146-1155, https://doi.org/10.1016/j.ijbiomac.2020.11.068.
[35] S. Sharma, P. Jain, S. Tiwari, Dynamic imine bond based chitosan smart hydrogel with magnified mechanical strength for controlled drug delivery, Int. J. Biol. Macromol., 160 (2020) 489-495, https://doi.org/10.1016/j.ijbiomac.2020.05.221.
[36] T. Sun, D. Zhou, F. Mao, Y. Zhu, Preparation of low-molecular-weight carboxymethyl chitosan and their superoxide anion scavenging activity, Eur. Polym. J., 43 (2007) 652-656, https://doi.org/10.1016/j.eurpolymj.2006.11.014.
[37] S. Dash, P.N. Murthy, L. Nath, P. Chowdhury, Kinetic modeling on drug release from controlled drug delivery systems, Acta Pol. Pharm., 67 (2010) 217-223.
[38] A.M. Craciun, L.M. Tartau, M. Pinteala, L. Marin, Nitrosalicyl-imine-chitosan hydrogels based drug delivery systems for long term sustained release in local therapy, Journal of Colloid and Interface Science, 536 (2019) 196-207, https://doi.org/10.1016/j.jcis.2018.10.048.
[39] B. Delley, From molecules to solids with the DMol 3 approach, The Journal of chemical physics, 113 (2000) 7756-7764, https://doi.org/10.1063/1.1316015.
[40] S. Grimme, J. Antony, S. Ehrlich, H. Krieg, A consistent and accurate ab initio parametrization of density functional dispersion correction (DFT-D) for the 94 elements

H-Pu, The Journal of chemical physics, 132 (2010) 154104, https://doi.org/10.1063/1.3382344.
[41] A. Klamt, G. Schüürmann, COSMO: a new approach to dielectric screening in solvents with explicit expressions for the screening energy and its gradient, Journal of the Chemical Society, Perkin Transactions 2, (1993) 799-805, https://doi.org/10.1039/P29930000799.
[42] N. Govind, M. Petersen, G. Fitzgerald, D. King-Smith, J. Andzelm, A generalized synchronous transit method for transition state location, Computational materials science, 28 (2003) 250-258, https://doi.org/10.1016/S0927-0256(03)00111-3.
[43] H.R. Rizvi, M.J. Khattak, A.A. Gallo, Rheological and mechanistic characteristics of Bone Glue modified asphalt binders, Construction Building Materials, 88 (2015) 64-73, https://doi.org/10.1016/j.conbuildmat.2015.03.023.
[44] R. Singh, K. Rao, A. Anjaneyulu, G. Patil, Moisture sorption properties of smoked chicken sausages from spent hen meat, Food Res. Int., 34 (2001) 143-148, https://doi.org/10.1016/S0963-9969(00)00145-9.
[45] P. Xue, N. Sun, Y. Li, S. Cheng, S. Lin, Targeted regulation of hygroscopicity of soybean antioxidant pentapeptide powder by zinc ions binding to the moisture absorption sites, Food Chem., 242 (2018) 83-90, https://doi.org/10.1016/j.foodchem.2017.09.025.
[46] J.B. Vaughn Jr, R.L. Stephens, R.E. Lenkinski, N.R. Krishna, G.A. Heavner, G. Goldstein, Proton NMR investigation of Ln3+ complexes of thymopoietin32–36, Biochimica et Biophysica Acta (BBA) - Protein Structure, 671 (1981) 50-60, https://doi.org/10.1016/0005-2795(81)90093-3.
[47] S. Li, A. El Ghzaoui, E. Dewinck, Rheology and drug release properties of bioresorbable hydrogels prepared from polylactide/poly (ethylene glycol) block copolymers, in: Macromol. Symp., Wiley Online Library, 2005, pp. 23-36, https://doi.org/10.1002/masy.200550403.
[48] N. Bhattarai, J. Gunn, M. Zhang, Chitosan-based hydrogels for controlled, localized drug delivery, Adv. Drug Del. Rev., 62 (2010) 83-99, https://doi.org/10.1016/j.addr.2009.07.019.
[49] S.V. Madihally, H.W. Matthew, Porous chitosan scaffolds for tissue engineering, Biomaterials, 20 (1999) 1133-1142, https://doi.org/10.1016/S0142-9612(99)00011-3.
[50] Y. Liang, X. Zhao, T. Hu, Y. Han, B. Guo, Mussel-inspired, antibacterial, conductive, antioxidant, injectable composite hydrogel wound dressing to promote the regeneration of infected skin, Journal of colloid interface science, 556 (2019) 514-528, https://doi.org/10.1016/j.jcis.2019.08.083.
[51] X. Lv, W. Zhang, Y. Liu, Y. Zhao, J. Zhang, M. Hou, Hygroscopicity modulation of hydrogels based on carboxymethyl chitosan/Alginate polyelectrolyte complexes and its application as pH-sensitive delivery system, Carbohydr. Polym., 198 (2018) 86-93, https://doi.org/10.1016/j.carbpol.2018.06.058.
[52] P. Gupta, K. Vermani, S. Garg, Hydrogels: from controlled release to pH-responsive drug delivery, Drug Discovery Today, 7 (2002) 569-579,

https://doi.org/10.1016/S1359-6446(02)02255-9.
[53] M.G. Bernengo, A. Appino, M. Bertero, M. Novelli, M.T. Fierro, G.C. Doveil, F. Lisa, Thymopentin in Sezary syndrome, JNCI: Journal of the National Cancer Institute, 84 (1992) 1341-1346, https://doi.org/10.1093/jnci/84.17.1341.
[54] A. Patruno, P. Tosco, E. Borretto, S. Franceschelli, P. Amerio, M. Pesce, S. Guglielmo, P. Campiglia, M.G. Bernengo, R. Fruttero, Thymopentin down-regulates both activity and expression of iNOS in blood cells of Sézary syndrome patients, Nitric Oxide, 27 (2012) 143-149, https://doi.org/10.1016/j.niox.2012.06.002.
[55] S. Zhao, M.M. Abu-Omar, Recyclable and malleable epoxy thermoset bearing aromatic imine bonds, Macromolecules, 51 (2018) 9816-9824, https://doi.org/10.1021/acs.macromol.8b01976.
[56] J. Siepmann, N.A. Peppas, Higuchi equation: derivation, applications, use and misuse, Int. J. Pharm., 418 (2011) 6-12, https://doi.org/10.1016/j.ijpharm.2011.03.051.

Biobased dynamic hydrogels by reversible imine bonding for controlled release of thymopentin

Rui Yu,[1] Eddy Petit,[1] Mihail Barboiu,[1*] Suming Li,[1*] Wenjing Sun,[2*] Congmei Chen[3]

[1] *Institut Européen des Membranes, IEM, UMR 5635, Univ Montpellier, CNRS, ENSCM, Montpellier, France*

[2] *China-America Cancer Research Institute, Key Laboratory for Medical Molecular Diagnostics of Guangdong Province, Guangdong Medical University, Dongguan, Guangdong 523808, China.*

[3] *National Supercomputing Center in Shenzhen (Shenzhen Cloud Computing Center), Guangdong, Shenzhen, 518055, China*

* Corresponding authors: suming.li@umontpellier.fr (S. Li); mihail-dumitru.barboiu@umontpellier.fr (M. Barboiu); swj_gdmc@163.com (W. Sun)

Abstract

Thymopentin (TP5) is widely used in the treatment of autoimmune diseases, but the short *in vivo* half-life of TP5 strongly restricts its clinical applications. A series of blank and TP5 loaded hydrogels were synthesized via reversible dual imine bonding by mixing water soluble *O*-carboxymethyl chitosan (CMCS) with a dynamer (Dy) prepared from Jeffamine and benzene-1,3,5-tricarbaldehyde. TP5 release from hydrogels was studied at 37°C under in vitro conditions. The molar mass of CMCS, drug loading conditions and drug content were varied to elucidate their effects on hydrogel properties and drug release behaviors. Density functional theory was applied to theoretically confirm the chemical connections between TP5 or CMCS with Dy. All hydrogels exhibited interpenetrating porous architecture with average pore size from 59 to 83 μm, and pH-sensitive swelling up to 10 000 % at pH 8. TP5 encapsulation affected the rheological properties of hydrogels as TP5 was partially attached to the network via imine bonding. Higher TP5 loading led to higher release rates. Faster release was observed at pH 5.5 than at pH 7.4 due to lower stability of imine bonds in acidic media. Fitting of release data using Higuchi model showed that initial TP5 release was essentially diffusion controlled. All these findings proved that the dynamic hydrogels are promising carriers for controlled delivery of hydrophilic drugs, and shed new light on the design of drug release systems by both physical mixing and reversible covalent bonding.

Keywords: *O*-carboxymethyl chitosan; Imine bonding; Dynamic hydrogel; Thymopentin; Drug release; Density functional theory

1. Introduction

Thymopentin (TP5) is a synthetic pentapeptide (Arg-Lys-Asp-Val-Tyr, M_n = 679.77) associated with the residual sequence (32-36) of thymic hormone thymopoietin [1, 2]. It possesses the biological properties characteristic of thymopoietin [3], and has been widely used for immunomodulation [4], and for treatments of autoimmune diseases [5], including cancer immunodeficiency [6], rheumatoid arthritis [7], tuberculosis [8], chronic heart failure [9], and chronic lymphocytic leukemia [10]. TP5 can facilitate the differentiation of thymocytes and affect the function to induce maturation of T-cells [11, 12] and bone marrow dendritic cells [13]. Nevertheless, due to the short half-life (≤ 30 s in plasma) and extensive metabolism in the gastrointestinal tract [14], TP5 is generally applied as a freeze-dried powder by intramuscular or percutaneous injection [5]. Chronic autoimmune diseases require long therapies and repetitive injections of TP5 which could provoke complications. These disadvantages highly limit the clinical utilization of TP5.

It has been reported that the in vivo efficiency of TP5 can be improved by slow infusion [15]. Therefore, controlled drug delivery systems are considered as an appealing strategy to achieve slow infusion of TP5, including nanoparticles [16], micelles [17], liposomes [18], and hydrogels [19, 20]. These various systems present many advantages such as prolonged drug release, constant drug concentration, reduced side effects, protection of drugs from degradation, etc. Micelles, liposomes and nanoparticles have been used to encapsulate TP5, but the encapsulation efficiency is quite low because of its high hydrophilicity [17, 21]. Dissolving microneedle array was studied as a new strategy for TP5 delivery by transdermal injection [4]. However, customized microneedle arrays and daily administration are needed, leading to high cost and low bioavailability. In contrast, hydrogel delivery systems appear most interesting for sustained delivery of hydrophilic drugs, and have been used clinically [22]. Hydrogels can easily encapsulate a variety of hydrophilic therapeutic agents, including small-molecule drugs [23], macromolecular drugs [24] and cells [25]. Furthermore, the high-water up taking capacity endows hydrogels with the physical features similar to tissues, and excellent biocompatibility. Besides, the crosslinked framework of hydrogels can hinder penetration of proteins [26], and thus protecting vulnerable bioactive drugs from degradation by inwardly diffusing enzymes [27].

Hydrogels have been investigated for the encapsulation of TP5. Zhang et al. developed

a physical hydrogel from polylactide-poly(ethylene glycol) (PLA-PEG) block copolymers via stereo-complexation between poly(L-lactide) and poly(D-lactide) blocks [19]. High drug loading and rapid drug release were obtained. Nevertheless, PLA degradation leads to acidic by-products which could provoke inflammatory reactions, and such physical hydrogels exhibit low stability and mechanical strength. Su et al. synthesized a hydrogel by crosslinking PLA grafted *O*-carboxymethyl chitosan (CMCS) using 1-(3-dimethylaminopropyl)-3-ethylcarbodiimide (EDC) and *N*-hydroxysuccinimide (NHS) as crosslinking agents [28]. The resulting hydrogel was used to encapsulate TP5 by immersion of dried gel in a TP5 solution. More than 80% of TP5 was released in 48 h. However, the presence of residual chemicals or solvents could compromise the biocompatibility of the system [29]. Therefore, it becomes a major challenge to develop a delivery system of TP5 which exhibits good biocompatibility, stability and high encapsulation efficiency.

CMCS is a water-soluble derivative of chitosan, the second most abundant polysaccharide in nature. It has been studied as a promising carrier for the delivery of peptides and proteins [30]. On the other hand, Jeffamine is a biocompatible polyetheramine containing poly(propylene oxide) (PPO) and poly(ethylene oxide) (PEO) blocks, as well as primary amino groups at chain ends. It has been used in drug delivery because of its water solubility and cytocompatibility [31]. Recently, our group has developed a CMCS and Jeffamine based dynamic hydrogel that could be potentially used for drug delivery [32], cartilage engineering [33], and antibacterial materials [34]. The hydrogel was prepared via dual imine bond crosslinking between the amino groups of CMCS and the aldehyde ones of a 3D dynamer (Dy). Dy was first obtained by Schiff-base reaction of 1,3,5-benzenetrialdehyde (BTA) and di-amino Jeffamine, followed by Schiff-base reaction of Dy and CMCS in aqueous solution to yield a 3D network. Trifunctional BTA served as a core to ensure 3D crosslinking, and Jeffamine as a linker to endow Dy with aqueous solubility. The gelation process is conducted in aqueous solution under mild conditions, which is beneficial for encapsulation of fragile drugs

such as proteins or peptides [22]. Different from other chitosan-based hydrogel by imine bonding [35], CMCS and Jeffamine based dynamic hydrogels exhibit regular and interconnected porosity which is beneficial for swelling, diffusion of physiological fluids, and drug encapsulation [33,34]. Interestingly, the hydrogel network contains free aldehyde and amino groups which are able to react with the functional groups of drugs or other bioactive molecules.

This work aimed to develop a novel delivery system of TP5 from CMCS and Jeffamine based dynamic hydrogels by in situ encapsulation. CMCS with different molar masses of CMCS was used since the molar mass affects the physico-chemical properties of hydrogels. *In situ* incorporation of TP5 within the dynamic hydrogel should allow to achieve complete drug encapsulation by physical adhesion to pore walls and reversible imine bonding to the hydrogel network via Schiff base reaction between the amino groups of TP5 and aldehydes of the dynamer. The rheological properties, internal morphology and swelling performance of dynamic hydrogels and TP5-loaded hydrogels were comparatively investigated. *In vitro* drug release of TP5-loaded hydrogels was studied under different conditions, and fitted using Higuchi's model. Finally, density functional theory (DFT) was applied to model the different imine bonds in the hydrogel network.

2. Experimental section

2.1 Materials

O,*O*'-bis(2-aminopropyl) poly(propylene glycol)-block-poly(ethylene glycol)-block-poly(propylene glycol), namely Jeffamine® ED-2003 with M_n of 1900, methanol (96%), hydrogen peroxide solution (H_2O_2, 30%) citric acid (99.5%), disodium hydrogen phosphate dodecahydrate (99%), boric acid (99.5 %), and borax (99%) were all of analytical grade, and obtained from Sigma-Aldrich. Benzene-1,3,5-tricarbaldehyde (BTA, purity 98%) was purchased from Manchester Organics. *O*-carboxymethyl chitosan (CMCS) with degree of carboxymethylation of 80 %, degree of deacetylation of 90 % was supplied by Golden-shell Biochemical Co., Ltd. TP5 (99%) was purchased from Soho-Yiming Pharmaceutical Co., LTD (Shanghai, China). All chemicals were

used as received without further purification.

2.2 Synthesis of dynamer

A dynamer (Dy) was synthesized from Jeffamine and BTA, as reported in our previous work [33]. Typically, BTA (81 mg, 0.5 mmol) and Jeffamine (0.95 g, 0.5 mmol) were dissolved in 20 mL methanol. The mixture was then heated to 70 °C and allowed to react for 4 h under gentle stirring. The solvent was totally removed by using rotary evaporator. 10 mL Milli Q water was added to yield a homogeneous Dy solution at a concentration of 0.05 M, as calculated from the remaining aldehyde groups.

2.3 Depolymerization of CMCS

Low molar mass CMCS was prepared via degradation of original CMCS in the presence of H_2O_2 [36]. Typically, CMCS (1 g) was dissolved in 30 mL Milli-Q water under stirring at 25 ℃. 0.15 mL H_2O_2 was then dropped in the solution. After 30 min degradation, the solution was immediately freezed by immersing in liquid nitrogen, and transferred onto a freeze dryer. After 24 h lyophilization, a white powder was obtained. The product was dissolved in 10 mL Milli-Q water, followed by precipitation in 200 mL absolute ethanol. Finally, the product was obtained by vacuum drying at 40℃ for 24 h. Another product was obtained after 60 min degradation using the same process. The M_n of original CMCS and depolymerized ones for 30 and 60 min are 80 000, 30 000 and 25 000, respectively, as determined by GPC in aqueous medium. They are accordingly named as CMCS80K, CMCS30K and CMCS25K.

2.4 Preparation of dynamic hydrogels

Dynamic hydrogels were prepared from CMCS, Jeffamine and BTA as previously reported [33, 34]. Typically, CMCS solution (0.15 M) was prepared by dissolving 0.318 g CMCS (1.5 mmol, calculated from D-glucosamine units) in 10 mL Milli-Q water at room temperature. The CMCS solution (0.15 M) was then mixed with the Dy solution

(0.05 M) with a 4/1 molar ratio of glucosamine/Dy. After removal of trapped bubbles by using ultra-sound, gelation was allowed to proceed at 37 ℃ for 24 h to yield a transparent hydrogel named as Gel80K, Gel30K or Gel25K according to the M_n of CMCS.

2.5 Preparation of TP5 loaded hydrogels

TP5 loaded hydrogels were prepared through *in situ* encapsulation. In brief, 2.625 mg TP5 was dissolved in 0.5 mL CMCS80K (0.15 M). The resulting solution was mixed with 0.375 mL Dy solution (0.05 M). The glucosamine of CMCS to Dy molar ratio was 4/1. After removal of bubbles, gelation then proceeded at 37 ℃ for 24 h to yield a TP5-loaded hydrogel with TP5 concentration of 3 mg/mL, namely Gel80K-TP5-3. Other TP5 loaded hydrogels were prepared using the same procedure but changing one parameter: Gel80K-TP5-0.1, Gel80K-TP5-9, Gel80K-TP5-3 (25°C) whose gelation occurred at 25°C, and Gel80K-TP5-3B prepared by dissolving TP5 in Dy solution before mixing with CMCS80K solution. TP5 was also loaded in Gel30K or Gel25K, and the corresponding samples were named as Gel30K-TP5-3 or Gel25K-TP5-3, respectively. In situ incorporation of TP5 results in complete drug encapsulation. Therefore, the drug loading capacity of all the TP5-loaded hydrogels is 100 %.

2.6 Characterization

^{1}H NMR spectroscopy was carried out using Bruker NMR spectrometer (400-LS) at 400 MHz. D_2O was used as the solvent. 5 mg of sample were dissolved in 0.5 mL of solvent for each analysis.

Gel permeation chromatography (GPC) was performed on a Water 1515 multidetector GPC system equipped with Waters 410 differential detector and ultra-hydrogel 250 column. 0.1 M NaCl was used as the mobile phase with a flow velocity of 0.6 mL/min. The column temperature was set at 40 ℃, and the sample concentration was 5.0 mg/mL. Poly(ethylene glycol) standards were used for calibration.

Fourier-transform infrared (FT-IR) spectroscopy of freeze-dried hydrogels was conducted on Nicolet Nexus FT-IR spectrometer, equipped with ATR diamant Golden Gate.

The morphology of freeze-dried hydrogels was examined by using Hitachi S4800 scanning electron microscopy (SEM). As-prepared hydrogels were placed in small vials, and immersed in liquid nitrogen (-196 °C) in order to conserve the original structure. The frozen samples were lyophilized with LABCONCO® freeze dryer for 24 h, and sputter coated prior to analysis.

Physical MCR 301 Rheometer (Anton Paar) was utilized to determine the rheological properties of hydrogels, using a cone plate geometry (diameter of 4 cm, apex angle of 2°, and clearance of 56 μm). The storage modulus (G′) and loss modulus (G″) were measured as a function of time, strain or frequency.

2.7 Swelling of freeze-dried hydrogels

The swelling performance of freeze-dried gels was evaluated by immersion in buffer solutions at different pH values. Buffers from pH 3 to pH 7.4 were prepared from 0.1 M citric acid and 0.2 M disodium hydrogen phosphate dodecahydrate solutions, buffers at pH 8 and pH 9 from 0.2 M boric acid and 0.05 M borax solutions, and buffer at pH 10 from 0.05 M borax and 0.2 M sodium hydroxide solutions. Freeze-dried gel samples were immersed in a buffer solution, and taken out after 24 h. The swollen hydrogels were weighed after wiping surface water with filter paper, and weighed again after 24 h lyophilization. The swelling and mass loss ratios of hydrogels were calculated according to the following equations:

$$\text{Swelling ratio } \% = \frac{(M_s - M_d)}{M_d} \times 100 \quad \text{(Eq. 1)}$$

$$\text{Mass loss ratio } \% = \frac{(M_0 - M_d)}{M_0} \times 100 \quad \text{(Eq. 2)}$$

Where M_0 is the initial mass of dried gel, M_s is the wet mass of the swollen hydrogel, and M_d is the dried mass of the swollen hydrogel after lyophilization.

2.8 *In vitro* release of TP5

In vitro drug release was realized in pH = 7.4 phosphate buffered saline (PBS) at 37 ℃. TP5-loaded hydrogel samples were placed in a centrifuge tube (50 mL) containing 10 mL pH 7.4 PBS. *In vitro* release was performed in shaking water bath at 37 ℃. At preset time intervals, 3 mL of the buffer solution were taken out, and replaced by 3 mL fresh buffer. TP5 concentration of the release supernatant was determined by HPLC-UV. A calibration curve was previously established using TP5 solutions with known concentrations. *In vitro* release of TP5 was also conducted in acidic buffer (pH 5.5), using the same procedure.

The cumulative release of TP5 was calculated using equation 3:

$$Release\ rate = \frac{V_e \sum_1^{n-1} C_i + V_0 C_n}{M_{drug}} \times 100 \quad \text{(Eq. 3)}$$

Where C_n and C_i represent the drug concentrations in the supernatant for n and i withdrawing steps, respectively; V_0 is initial total volume of PBS; V_e is collected volume of PBS; M_{drug} is the original loading amount of TP5. The drug loading efficiency is 100 % due to the *in situ* encapsulation of TP5. All of the experiments were performed in triplicate, and values were given in mean ± SD for n = 3.

2.9 The release kinetics model

The release kinetics of the various TP5-loaded hydrogel systems were studied by fitting the *in vitro* release data using Higuchi's model [37, 38]:

$$Q_t = K_H \times t^{\frac{1}{2}} \quad \text{(Eq. 4)}$$

where Q_t is the quantity of drug released within the time t, K_H is the Higuchi dissolution constant.

2.10 Density functional theory (DFT) computation

All calculations were performed using the Dmol^3 code in the Materials Studio 7.0 package [39]. The GGA/PBE functional was selected, and double numerical plus polarization (DNP) was used as the basis set [40]. Convergence tolerances for the total

energy, maximum force, and maximum displacement were set to 1.0×10^{-5} Hartree, 2.0×10^{-3} Hartree/Å, and 5.0×10^{-3} Hartree/Å, respectively. The self-consistent field convergence was 1.0×10^{-6} Hartree. To accelerate the self-consistent field (SCF) convergence, the smearing was set to 0.005 Hartree. The solvent effect was simulated by conductor-like screening model (COSMO) [41], using the dielectric constant of 78.54 (water). The transition states were calculated by using the synchronous method with conjugated gradient refinements. This method involves linear synchronous transit (LST) maximization, followed by repeated conjugated gradient (CG) minimizations, then quadratic synchronous transit (QST) maximizations and repeated CG minimizations until a transition state is located [42]. The energy barrier ($E_{Barrier}$) was calculated using equation 5:

$$E_{Barrier} = E_{TS} - E_{IN} \quad \text{(Eq. 5)}$$

where E_{TS} is the energy of the transition state, and E_{IN} the energy of the intermediate connected to the transition state.

The reaction energy (E_{RE}) of the elementary steps was calculated using equation 6:

$$E_{RE} = E_P - E_R \quad \text{(Eq. 6)}$$

where E_P is the energy of the elementary reaction product, and E_R the initial energy of the elementary reaction reactant.

3. Results and discussion

3.1 Preparation of hydrogels

Dynamic hydrogels were synthesized via Schiff-base reaction between CMCS and the dynamer, as shown in Scheme 1. Upon mixing CMCS and Dy aqueous solutions, the amino groups along the CMCS backbone react with the remaining aldehyde groups of Dy, resulting in formation of a 3D hydrogel network by dual imine bonding. The CMCS to Dy molar ratio of 4:1 was adopted since it allows optimal crosslinking, as demonstrated in our previous work [33]. In situ TP5 encapsulation in hydrogels is also shown in Scheme 1. Table 1 summarizes all the details for the preparation of blank and

drug loaded hydrogels.

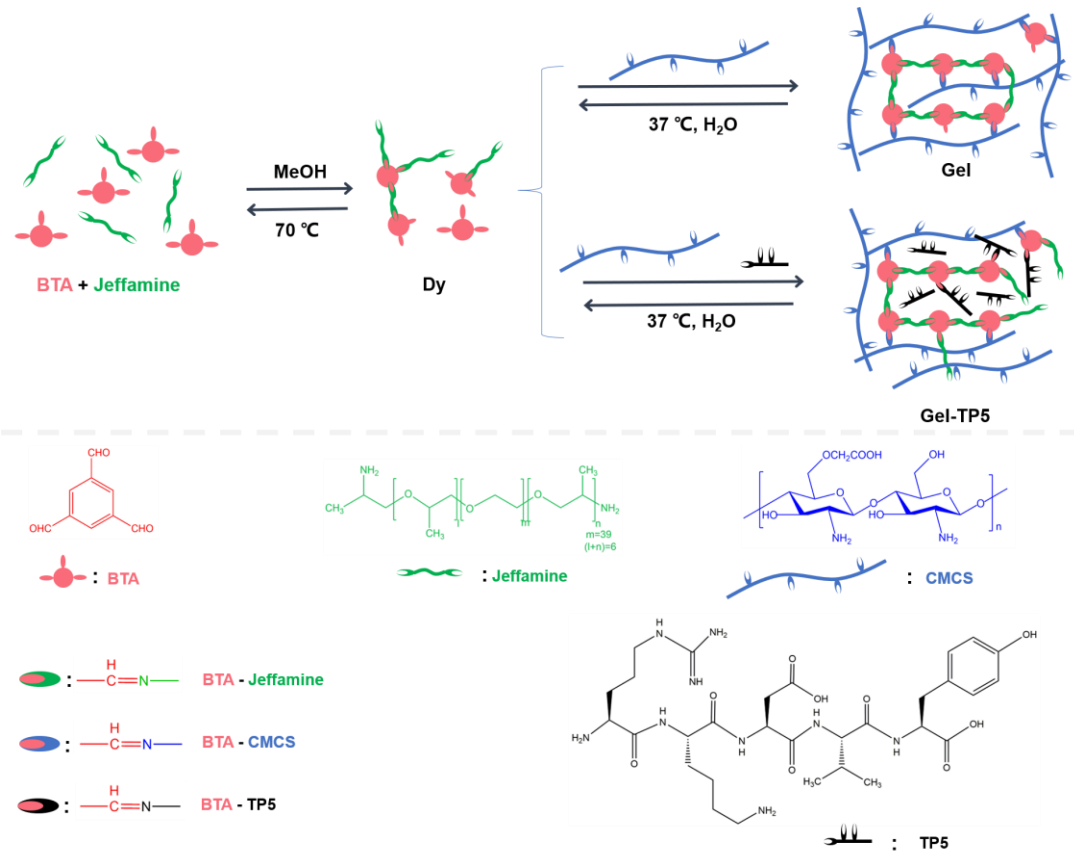

Scheme 1. Synthesis of dynamic hydrogels via Schiff-base reaction between CMCS and Dy, and in-situ loading of TP5 in hydrogels.

Table 1. Molar and mass compositions of blank and TP5 loaded hydrogels [a)]

Sample	CMCS80K		CMCS30K		CMCS25K		Dy [c)]		TP5 [f)]
	[mmol] [b)]	[w/v%]	[mmol] [b)]	[w/v%]	[mmol] [b)]	[w/v%]	[mmol]	[w/v%]	[mg/mL]
Gel80K	0.3	1.8	-	-	-	-	0.075	4.3	-
Gel30K	-	-	0.3	1.8	-	-	0.075	4.3	-
Gel25K	-	-	-	-	0.3	1.8	0.075	4.3	-
Gel80K-TP5-0.1	0.3	1.8	-	-	-	-	0.075	4.3	0.1

Gel80K-TP5-3	0.3	1.8	-	-	-	-	0.075	4.3	3
Gel80K-TP5-3B [d]	0.3	1.8	-	-	-	-	0.075	4.3	3
Gel80K-TP5-3 (25 ℃) [e]	0.3	1.8	-	-	-	-	0.075	4.3	3
Gel80K-TP5-9	0.3	1.8	-	-	-	-	0.075	4.3	9
Gel30K-TP5-3	-	-	0.3	1.8	-	-	0.075	4.3	3
Gel25K-TP5-3	-	-	-	-	0.3	1.8-	0.075	4.3	3

a) Hydrogels were prepared by mixing the aqueous solutions of 0.15 M CMCS80K/CMCS30K/CMCS25K and 0.05 M Dy at a D-glucosamine/Dy molar ratio of 4/1 (total volume of 3.5 mL), TP5 loaded hydrogels were prepared by adding TP5 in CMCS solution before mixing with Dy solution; b) Moles of glucosamine units of CMCS. Calculations were made on the basis of the average molar mass of 212 g/mol obtained for D-glucosamine, taking into account the degree of deacetylation of 90% and the degree of carboxymethylation of 80%; c) The concentration of Dy solution was obtained from the remaining aldehyde groups. In a typical reaction, 0.5 mmol BTA (81 mg) reacted with 0.5 mmol Jeffamine ED2003 (950 mg) to form a Dy solution. As BTA had 3 aldehydes and Jeffamine 2 amines, there remained theoretically 0.5 mmol of aldehydes in the dried Dy. Addition of 10 mL water yielded a dynamer solution of 0.05 M. d) Gel80K-TP5-3B was prepared by adding TP5 in Dy solution before mixing with CMCS solution e) Gel80K-TP5-3 (25 ℃) was prepared at 25 ℃; f) The concentration of TP5 in hydrogel was 0.1 mg/ml or 3 mg/ml or 9 mg/ml.

3.2 FT-IR and NMR

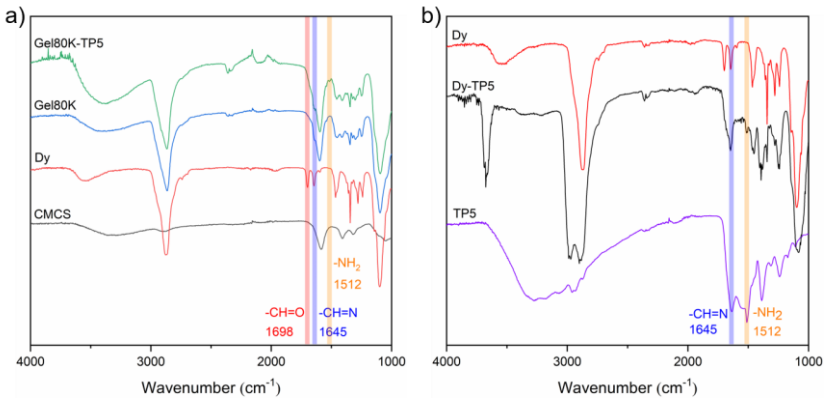

Fig. 1. a) FT-IR spectra of freeze-dried CMCS, Dy, Gel80K and Gel80K-TP5-3; b) FT-IR spectra of Dy, TP5, and Dy-TP5 which is an obtained by mixing TP5 in Dy solution at a molar ratio of 1/1, reaction at 37℃ for 24h, and 24 h lyophilization.

Fig. 1a shows the FTIR spectra of CMCS, Dy, freeze dried Gel80K and TP5 loaded

Gel80K-TP5-3. CMCS presents a large band around 3350 cm^{-1} which is attributed to free OH and NH_2 groups, and an intense band at 1595 cm^{-1} due to carbonyl groups. The dynamer exhibits two intense bands at 2850 and 1100 cm^{-1} assigned to C-H and C-O stretching, and two characteristic bands at 1698 and 1645 cm^{-1} corresponding to aldehyde and imine bonds, respectively. All the characteristic bands of CMCS and Dy are observed on the spectrum of freeze dried Gel80K. Nevertheless, the band of aldehyde groups at 1698 cm^{-1} is almost invisible, but the band at 1645 cm^{-1} corresponding to newly formed imine bonds is clearly distinguished. These results illustrate that hydrogels are formed due to imine formation between aldehydes of Dy and amine groups of CMCS. On the spectrum of Gel80K-TP5-3, a band is detected at 2100 cm^{-1}, which is assigned to the O-H stretching of water [43]. In fact, the freeze-dried samples rapidly absorbed water due to the high hygroscopicity of TP5 [44, 45]. Similar findings are obtained for other blank and TP5 loaded hydrogels (Fig. S1).

Fig. 1b presents the FT-IR spectra of Dy, TP5 and a Dy-TP5 mixture. The latter was prepared in order to figure out the reactions between the aldehydes of Dy and the amines of TP5. It was obtained by dissolving TP5 in Dy solution at a molar ratio of 1/1, followed by 24 h reaction at 37 ℃ and finally 24 h lyophilization. TP5 presents characteristic bands at 1630 and 1512 cm^{-1} which are assigned to the C=O stretching of amides and N-H pending of amines, together with a large band around 3300 cm^{-1} due to the presence of water. Interestingly, the band of aldehydes at 1698 cm^{-1} is not detected on the spectrum of Dy-TP5, suggesting that the aldehydes have reacted with the amine groups of TP5 via Schiff-base reaction.

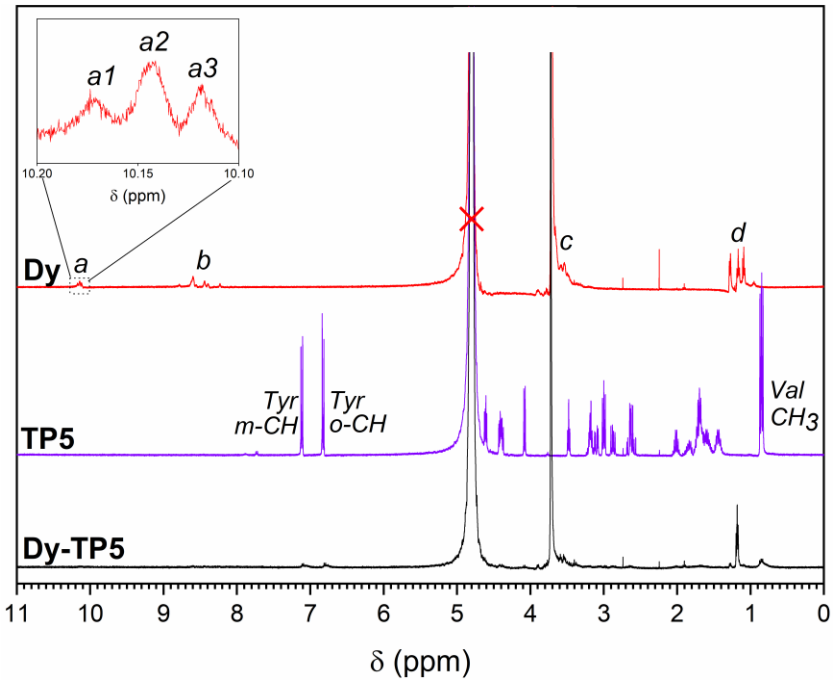

Fig. 2. ^{1}H NMR spectra of the Dy, TP5, and Dy-TP5 in D_2O.

Fig. 2 shows the ^{1}H NMR spectra of the Dy, TP5, and Dy-TP5. On the spectrum of Dy, the three small signals in the 10.1-10.2 ppm range are assigned to aldehyde groups of BTA with different degrees of substitution, including non-substituted (a1), mono-substituted (a2), and di-substituted aldehydes (a3). Signals between 8.2 and 8.7 ppm belong to the aromatic protons of BTA and imine protons (b). Signals around 3.7 ppm are assigned to the methylene and methine protons (c) of Jeffamine, and signals between 1.0 and 1.3 ppm to the methyl protons (d) of Jeffamine [33, 34]. The presence of residual H_2O is detected at 4.8 ppm. TP5 presents numerous signals associated to the various protons of the pentapeptide (Arg-Lys-Asp-Val-Tyr). The two doublets around 7.15 and 6.85 ppm are assigned to the meta-CH (Tyr m-CH) and ortho-CH (Tyr o-CH) on the phenyl ring of tyrosine [46], respectively. The three signals between 4.0 and 4.7 ppm belong to the various methine protons, and the signals between 1.3 and 3.6 ppm to the various methylene protons of the pentapeptide. The strong signal at 0.85 ppm is attributed to the methyl protons of valine (Val CH_3) [46]. Importantly, no signals in the range of 10.1-10.2 ppm are observed on the spectrum of Dy-TP5, implying that all the remaining aldehydes of Dy have completely reacted with the amine groups of TP5, in

agreement with FTIR data (Fig. 1b).

The morphology of CMCS, Dy, their mixtures with TP5 (CMCS-TP5 and Dy-TP5) was examined by using SEM (Fig. S2). No obvious difference is observed between pristine CMCS (Fig. S2a, b) and CMCS-TP5 (Fig. S2e, f). Both samples display a lamellar structure with the presence of holes of *c.a* 10 µm, suggesting the absence of interactions between the two components. In contrast, difference is detected between pristine Dy (Fig. S2c, d) and the mixture Dy-TP5 (Fig. S2g, h). Both samples exhibit a highly porous structure. The surface of Dy appears rugged, whereas that of Dy-TP5 appears smooth. These findings seem to indicate the occurrence of interactions between TP5 and the Dy.

3.3 Rheology

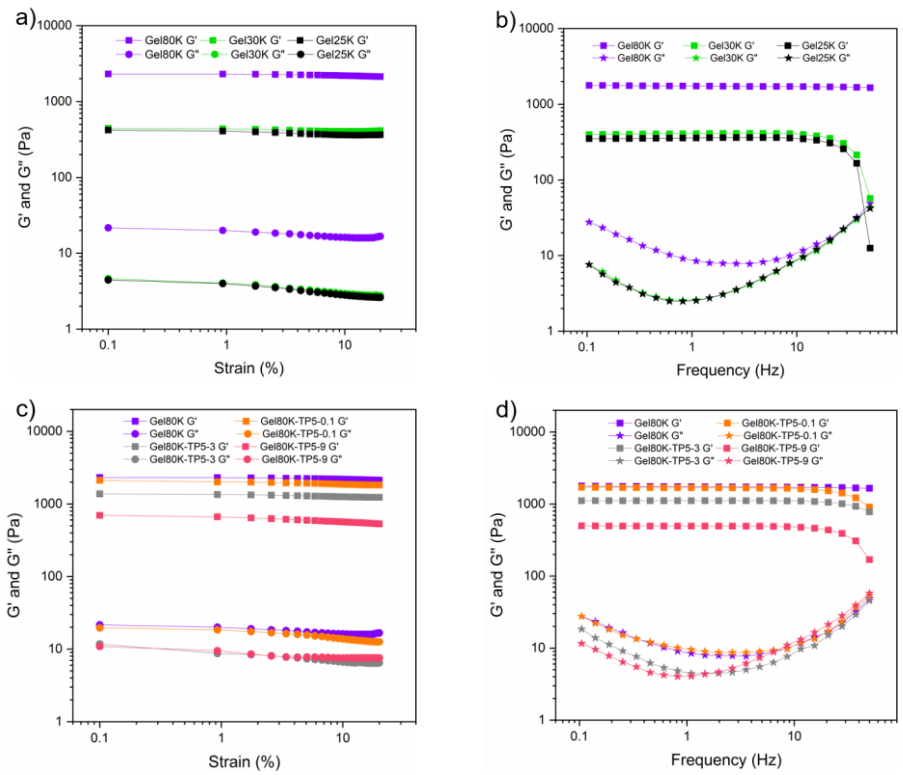

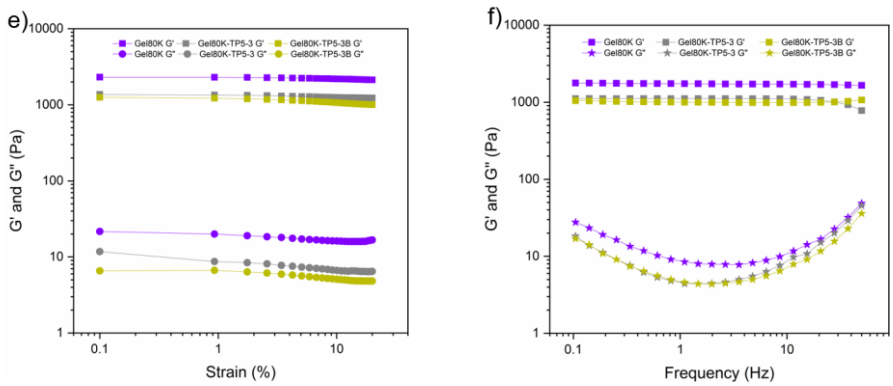

Fig. 3. Storage modulus (G′) and loss modulus (G″) changes of Gel80K, Gel30K and Gel25K as a function of strain at 25 °C and at 1 Hz (**a)** and as a function of frequency at 25 °C and at a strain of 1 % (**b)**; G′ and G″ changes of Gel80K, , Gel80K-TP5-0.1, Gel80K-TP5-3 and Gel80K-TP5-9 as a function of strain at 25 °C and at 1 Hz (**c)** and as a function of frequency at 25 °C and at a strain of 1% (**d)**; G′ and G″ changes of Gel80K, Gel80K-TP5-3, and Gel80K-TP5-3B as a function of strain at 25 °C and at 1 Hz (**e)** and as a function of frequency at 25 °C and at a strain of 1 % (**f)**.

Rheological measurements were conducted on the various hydrogels at 25 °C to evidence the effect of CMCS molar mass on the rheological properties as well as the interaction between TP5 and Dy in the hydrogel network. Firstly, the storage modulus (G′) and loss modulus (G″) changes of blank hydrogels (Gel80K, Gel30K and Gel25K) were determined as a function of strain at a frequency of 1 Hz and at 25 °C, as shown in Fig. 3a. As the strain increases from 0.1 % to 20 %, G′ remains almost constant for all the blank hydrogels, whereas G″ slightly decreases, indicating a linear viscoelastic (LVE) behavior of hydrogels in the 0.1 to 20 % strain range. Meanwhile, the moduli of blank hydrogels are highly dependent on the molar mass of CMCS. With the decrease of molar mass of CMCS from 80,000 to 30,000 and to 25,000, G′ at a strain of 1% decreases from 2300 Pa for Gel80K to 440 Pa for Gel30K, and to 420 Pa for Gel25K, respectively. Similar phenomena are observed for G″ changes. In fact, higher molar mass chains have more amino groups, which allows to enhance the crosslinking density, thus resulting in higher modulus of hydrogels

Fig. 3b shows the modulus changes of blank hydrogels as a function of frequency from 0.1 Hz to 50 Hz at a constant strain (1%) and at 25 °C. G′ remains constant in the whole frequency range for Gel80K, whereas a sharp decrease of G′ is observed beyond 30 Hz in the cases of Gel30K and Gel25K. On the other hand, G″ exhibits some fluctuations with increasing frequency. These rheological results well corroborate with the formation of highly stable covalent networks, in contrast to physical hydrogels whose storage and loss moduli increase with increasing frequency due to chain entanglements [19, 47]. It is also noteworthy that Gel80K exhibit higher stability than Gel30K and Gel25K due to higher crosslinking density as mentioned above.

Fig. 3c presents G′ and G″ changes *versus* strain of Gel80K hydrogels containing various amounts of TP5 (0, 0.1, 3, and 9 mg/mL). Obviously, with addition of TP5 in hydrogels, G′ decreases from 2310 Pa for Gel80K to 2222 Pa for Gel80K-TP5-0.1, to 1374 Pa for Gel80K-TP5-3, and to 697 Pa for Gel80K-TP5-9. These results illustrate that *in situ* TP5 encapsulation affects the rheological properties of drug loaded hydrogels. In fact, the amine groups of TP5 can react with the free aldehyde groups of Dy, as shown in Fig. 1b and Fig. 2. Hence, there is competition between TP5 and CMCS after mixing aqueous solution of Dy with that of CMCS and TP5, leading to decreased imine bonding between CMCS and Dy. On the other hand, attachment of TP5 to the network does not contribute to the crosslinking because TP5 is a small molecule compared to CMCS. Therefore, the crosslinking density decreases with increase of TP5 content, and consequently the modulus of hydrogels decreases. A frequency sweep of hydrogels was performed over a range from 0.01 to 50 Hz at a fixed strain of 1 %. G′ remains constant for Gel80K, and slightly decreases beyond 30 Hz for TP5 loaded hydrogels, indicating that TP5 encapsulation affects the stability of hydrogels.

A hydrogel (Gel80K-TP5-3B) was prepared by dissolving TP5 in Dy solution, followed by mixing with CMCS solution before gelation. As TP5 is supposed to react with Dy, dissolving TP5 in Dy solution should favor imine formation between them. G′ and G″ changes of Gel80K, Gel80K-TP5-3, and Gel80K-TP5-3B were examined as a

function of strain and frequency (Fig. 3e, f). Noticeably, G′ of Gel80K-TP5-3 is higher than that of Gel80K-TP5-3B in nearly the whole strain and frequency ranges, which confirms that mixing TP5 and Dy first decreased the crosslinking density of hydrogels. Strain and frequency sweeps were also performed on blank and TP5 loaded Gel30K and Gel25K hydrogels (Fig. S3). Similar phenomena were observed, illustrating the stability of hydrogels and interactions between TP5 and the dynamer.

3.4 Morphology and swelling properties

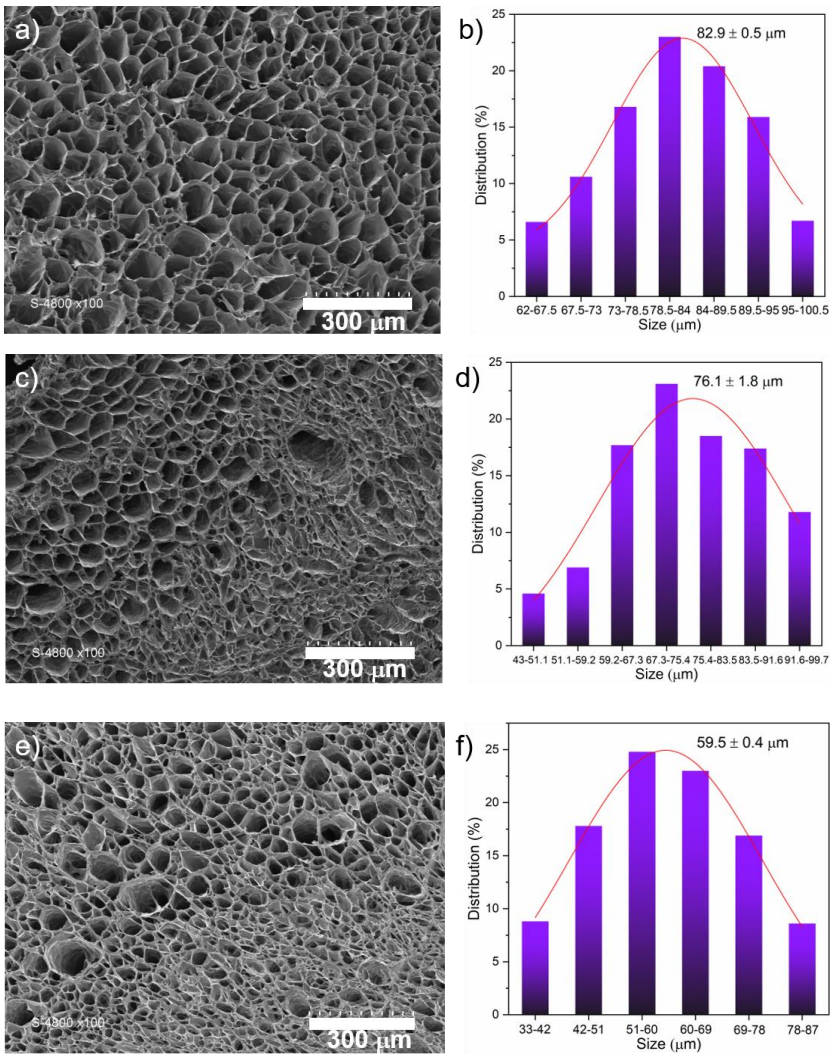

Fig. 4. SEM images and pore size distributions of freeze-dried gels: (a, b) Gel80K; (c, d) Gel30K; (e, f) Gel25K.

The morphology of as-prepared hydrogels after lyophilization was observed by SEM. Obviously, all hydrogels exhibit interpenetrating and porous architectures. Compared to Gel30K and Gel25K, Gel80K displays more regular structure and narrower distribution of interconnected pores (Fig. 4a). The average pore diameter of Gel80K, Gel30K and Gel25K is 82.9 ± 0.5 μm (Fig. 4b), 76.1 ± 1.8 μm (Fig. 4d), and 59.5 ± 0.4 μm (Fig. 4f), respectively. Thus, it seems that the pore diameter slightly decreases with decrease of the molar mass of CMCS. Moreover, in a previous work, it was shown that the pore diameter of dynamic hydrogels is dependent on the molar mass of Jeffamine linker [34]. Therefore, the porous structure of dynamic hydrogels can be tailored by varying the molar mass of the components. On the other hand, the interconnected porous structure enables hydrogels to mimic the extracellular matrix, which is beneficial for biomedical applications in drug delivery [48], and in tissue engineering [33, 49]. Therefore, Gel80K which has the optimal porous "spongy" characteristics was selected as the carrier of an in-depth study of drug release.

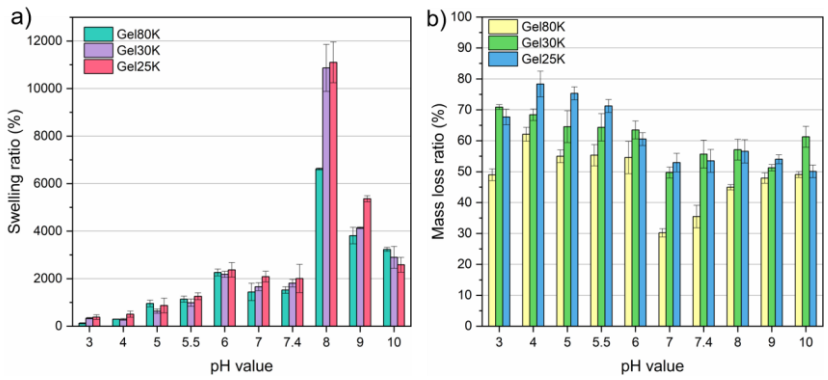

Fig. 5. a) Swelling ratios, and b) Mass loss ratios of Gel80K, Gel30K and Gel25K after 24 h immersion in buffers at various pH values. Data are expressed as mean ± SD for n = 3.

As aforementioned, the most important characteristic of hydrogels is their capability to retain large amount of water in the polymeric network, which is beneficial for controlling the release profiles of drugs and the absorption of wound exudate [50]. Fig. 5a presents the swelling performance of freeze-dried hydrogels in buffers at various pH

values. All the hydrogels exhibit a highly pH-dependent swelling behavior. The swelling degree is relatively low (< 1000 %) in strong acid buffers (pH 3/4), and increases to around 2000 % from pH 4 to 6. It remains at the same level around 2000 % in the pH 6 to 7.4 range. All hydrogels exhibit a maximum swelling at pH 8, 6600 % for Gel80K, 10000 % for Gel30K, and 11000 % for Gel25K. As the alkalinity continues to increase to pH 9 and 10, the swelling degree of hydrogel deceases dramatically to a level around 3000 %. In addition, there is no major difference between the swelling ratios of the three samples except at pH 8. The pH sensitivity of the swelling of hydrogels is assigned to electrostatic interactions between the amino and carboxyl groups along CMCS chains [33, 51]. In fact, the pK_a of amino and carboxyl groups of CMCS is 6.5 and 2.7, respectively. Contraction of hydrogels occurs because of strong electrostatic attraction between negatively charged -COO^- and positively charged -NH_3^+ groups which result from protonation in strong acidic media (pH 3 and 4), thus leading to low swelling ratio. Electrostatic attraction diminishes with the decrease of the H^+ concentration (pH 5, 5.5, and 6), and thus the swelling gradually increases. At pH 6, 7 and 7.4 which are around the pK_a of amino groups, the swelling remains almost constant as the electrostatic interactions are weak due to low concentrations of charges. In contrast, high swelling of hydrogels occurs because of strong repulsion between negatively charged -COO^- groups at pH 8. Nevertheless, with higher alkalinity at pH 9 and 10, OH^- ions in solution would counterbalance the electrostatic repulsion between -COO^- groups [33], thus resulting in decrease of the swelling degree. The pH sensitive swelling of hydrogels could be of great importance for the design of drug delivery systems due to large variation of physiological pH at various body sites in normal and pathological conditions [52].

Mass loss of hydrogels occurs during the swelling process due to the solubilization and washing away of non-crosslinked species, as shown in Fig. 5b. Overall, the mass loss ratio of all the hydrogels varies between 30 % and 80 % in the whole pH range. The hydrogels show higher mass loss in acid conditions than in neutral and alkaline

conditions. Noticeably, the mass loss ratio of Gel80K is lower than those of Gel30K and Gel25K in the whole pH range. This finding could be attributed to the better cross-linking Gel80K as compared to Gel30K and Gel25K because Gel80K was prepared from CMCS80K with higher molar mass, in agreement with rheological data. The lowest mass loss ratio is 30 and 36 % obtained for Gel80K at pH 7 and 7.4, respectively, in agreement with the better stability of Gel80K at neutral pH. Thus, Gel80K is used for a comprehensive study of TP5 release from hydrogels under various conditions.

The swelling and mass loss behaviors of Gel80K were investigated under drug release conditions in pH 7.4 PBS at 37 ℃ up to 168 h (Fig. S4, Information supplementary). The swelling ratio rapidly increases to 750 % and 1200 % after immersion for 10 and 20 min, respectively, whereas the mass loss ratio increases 25 % and 32 % in the meantime. Thereafter, the swelling and mass loss ratios remain almost at the same level up to 168 h, fluctuating around 1300 % and 34 %, respectively. These findings indicate that an equilibrium is rapidly reached after immersion of dried gels in PBS, and that the hydrogels are stable after initial mass loss.

3.5 *In vitro* release of the TP5

TP5 is an immuno-modulating drug, and is widely applied in the treatment of autoimmune diseases such as chronic lymphocytic leukemia [10], Sezary's syndrome [53, 54], etc. Besides, TP-5 is able to induce the differentiation of T-cells and accelerate the development of T lymphocytes [11]. A series of TP5-loaded hydrogels were prepared, including Gel80K-TP5-0.1, Gel80K-TP5-3, Gel80K-TP5-9, Gel80K-TP5-3B, Gel80K-TP5-3(25°C), Gel30K-TP5-3, and Gel25K-TP5-3 so as to evaluate the effects of various factors.

The morphology of the various TP5-loaded hydrogels was examined by using SEM (Fig. S5). It appears that TP5 encapsulation affects the regularity of the porous structure of hydrogels. In fact, Gel80K-TP5-0.1 exhibits a porous structure similar to that of Gel80K (Fig. 4a,b), but the surface appears rougher. With increase of TP5 content from

0.1 mg/mL (Fig. S5a, b) to 3 mg/mL (Fig. S5c, d), and to 9 mg/mL (Fig. S5e, f), the three-dimensional architecture becomes more and more irregular as compared with that of Gel80K (Fig. 4a,b). Similarly, TP5 encapsulation also affects the structure of Gel30K-TP5-3 (Fig. S5i, j) and Gel25K-TP5-3 (Fig. S5k, l) as compared to corresponding blank hydrogels. On the other hand, difference is also noticed between the morphology of Gel80K-TP5-3 and Gel80K-TP5-3B (Fig. S5g, h). Both have exactly the same compositions, but different mixing orders. Gel80K-TP5-3B exhibits a smoother surface compared to Gel80K-TP5-3.

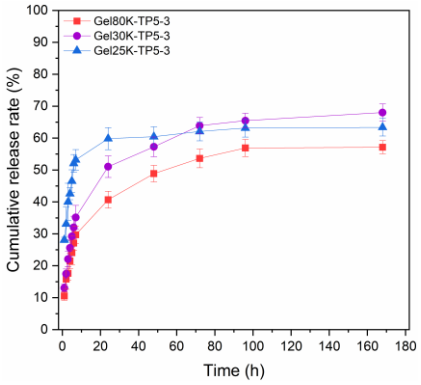

Fig. 6. Cumulative release of TP5 from Gel80K-TP5-3, Gel30K-TP5-3, and Gel25K-TP5-3. Values were expressed as mean ± SD for n = 3.

TP5 release from the various TP5-loaded hydrogels was monitored to evaluate the potential of dynamic hydrogels as drug carrier in cancer therapy [38]. Fig. 6 shows the release profiles of TP5 from Gel80K-TP5-3, Gel30K-TP5-3, and Gel25K-TP5-3 in pH 7.4 PBS at 37 ℃. Overall, all samples displayed a release profile in two stages, namely a burst release in the first 7 h followed by a slow and continuous release during 7 days. After 1 h in the medium, significant release rates are recorded, 28.0% for Gel25K-TP5, 13.0 % for Gel30K-TP5 and 10.5 % for Gel80K-TP5. TP5 release increases almost linearly to reach 53.2 %, 35.1 % and 29.7 % after 7 h for the 3 samples, respectively. Thereafter, TP5 release slows down, reaching a plateau after 96 h. The total TP5 release is 63.4, 68.0, and 57.1% after 168 h for Gel25K-TP5, Gel30K-TP5 and Gel80K-TP5, respectively. Gel80K-TP5 exhibits slower and more sustainable release as compared to

Gel25K-TP5 and Gel30K-TP5 due to its higher crosslinking density which disfavors drug diffusion. Therefore, Gel80K is used as drug carrier in further studies.

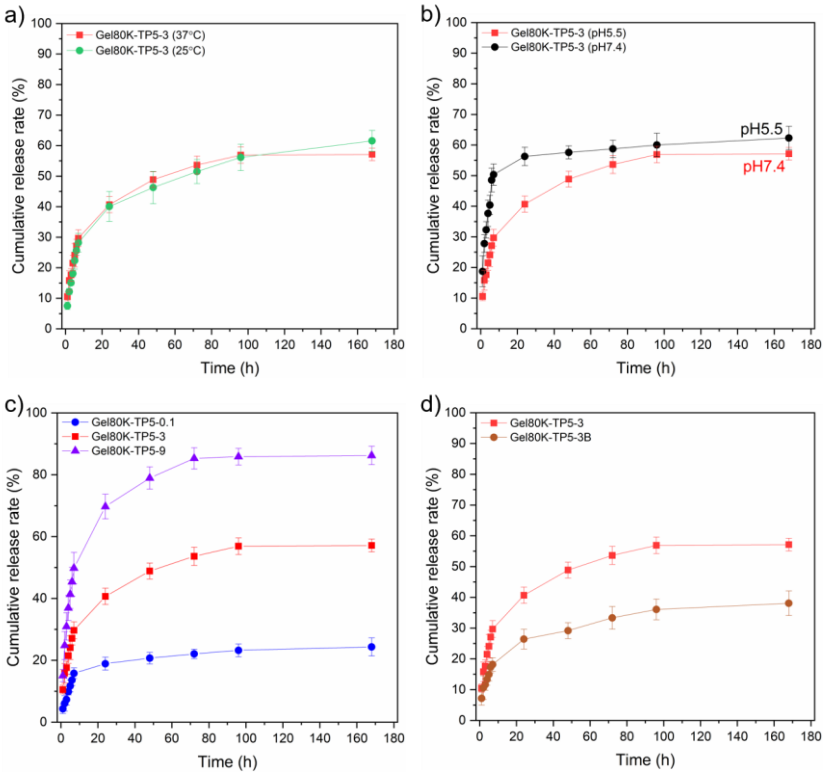

Fig. 7. a) Cumulative release of TP5 from Gel80K-TP5-3 prepared at 25 ℃ and 37 ℃, namely Gel80K-TP5-3 (25 ℃) and Gel80K-TP5-3 (37 ℃); b) Cumulative release of TP5 from Gel80K-TP5-3 in PBS at pH 7.4, and in acid buffer medium at pH 5.5, namely Gel80K-TP5-3 (pH 7.4) and Gel80K-TP5-3 (pH 5.5); c) Cumulative release of TP5 from Gel80K loaded with various TP5 contents: Gel80K-TP5-0.1, Gel80K-TP5-3, and Gel80K-TP5-9; d) Cumulative release of TP5 fromGel80K-TP5-3 and Gel80K-TP5-3B with different mixing orders. Values were expressed as mean ± SD for n = 3.

Fig. 7 show the TP5 release curves from various hydrogels. No difference is noticed between the release profiles Gel80K-TP5-3 prepared at 25 °C and at 37 °C (Fig. 7a), indicating the gelation temperature (25 or 37 °C) of Gel80K-TP5 has little impact on the release of TP5. In contrast, faster initial release is observed from Gel80K-TP5-3 at pH 5.5 than at pH 7.4, although both present similar equilibrium release ratios around

60% (Fig. 7b). This difference can be assigned to the fact that the imine bonds are prone to hydrolysis under acidic condition [55], which leads to partial disassociation of the three-dimensional hydrogel network thus favoring the diffusion of trapped TP5. It is also of interest to evaluate the effect of initial drug load on the release rate by comparing the release profiles of Gel80K-TP5-0.1, Gel80K-TP5-3, Gel80K-TP5-9, as shown in Fig. 7c. Apparently, the latter shows the highest equilibrium rate, reaching 90 % after 168 h, which is much higher than that of Gel80K-TP5-0.1 (22.5%) and Gel80K-TP5-3 (57 %). This difference well corroborates with the partial attachment of TP5 to the hydrogel network by imine bonding. It can be assumed that only free TP5 is released as imine bonds are stable at pH 7.4. Thus, hydrogels with higher drug loading have higher proportion of free drug, and consequently present higher drug release ratio [38]. Finally, TP5 release behaviors from Gel80K-TP5-3 and Gel80K-TP5-3B are compared to examine the effect of the mixing order (Fig. 7d). Gel80K-TP5-3B presents a total release ratio of 38%, which is much lower than that of Gel80K-TP5-3 (60%). This finding also confirms the covalent attachment of TP5 to the hydrogel network by imine bonding. As TP5 is first mixed with Dy before mixing with CMCS in the case of Gel80K-TP5-3B, more TP5 is covalently attached to the network, leading to lower TP5 release as compared to Gel80K-TP5-3. These data indicate that only physically encapsulated TP5 can be released under in vitro conditions. The release rate of TP5 from hydrogels depends on many factors such as the molar mass of CMCS, the pH of the medium, the drug load, and the mixing order during hydrogel preparation.

3.6 Drug release kinetics

Table 2 Parameters obtained from fitting of experimental data using Higuchi model [a)]

Sample	R^2	K_H
Gel80K-TP5-0.1	0.967	6.477
Gel80K-TP5-3	0.990	11.110
Gel80K-TP5-9	0.998	20.897

Gel80K-TP5-3B	0.978	6.502
Gel80K-TP5 (pH5.5)	0.982	19.141
Gel80K-TP5 (25℃)	0.985	12.271
Gel30K-TP5	0.997	13.315
Gel25K-TP5	0.986	16.172

a) Experimental data in Fig. 6-7.

It is widely admitted that the release of a hydrophilic drug from a monolithic matrix mainly depends on the diffusion process. Other factors such as physical forces between the drug and the hydrogel matrix and swelling of bulk hydrogel affect the release profile as well. Higuchi's model has been largely used to describe the drug release kinetics of various systems. It is based on the Fick's Law where the release proceeds by the diffusion of drugs through the delivery system. In this case, the cumulative released drug amount is proportional to the square root of time. TP5 release kinetics were investigated by fitting of experimental data in the first 6 h using Higuchi model in order to better understand the release mechanism of TP5 from dynamic hydrogels [38], as shown in Fig. S6 and Table 2.

Data in Table 2 show that the correlation coefficient is above 0.98 in all cases except Gel80K-TP5-0.1, suggesting that the TP5 release was mainly controlled by diffusion process [56]. In fact, the maximum concentration of TP5 after total release in the release medium is well below its saturation concentration (> 10 mg/mL) even for Gel80K-TP5-9 [19]. Thus, it could be considered that the dissolution is the ruling force of TP5 release from the hydrogels as drug release was conducted under immersion conditions [38]. It is also of interest to compare the K_H values of the different systems. Gel80K-TP5-9 and Gel80K-TP5-0.1 present the highest and the lowest K_H values, respectively, in agreement with the fastest and the slowest release rates. Intermediate K_H values were obtained for other TP5 loaded hydrogels.

3.7 Density functional theory (DFT) modelling

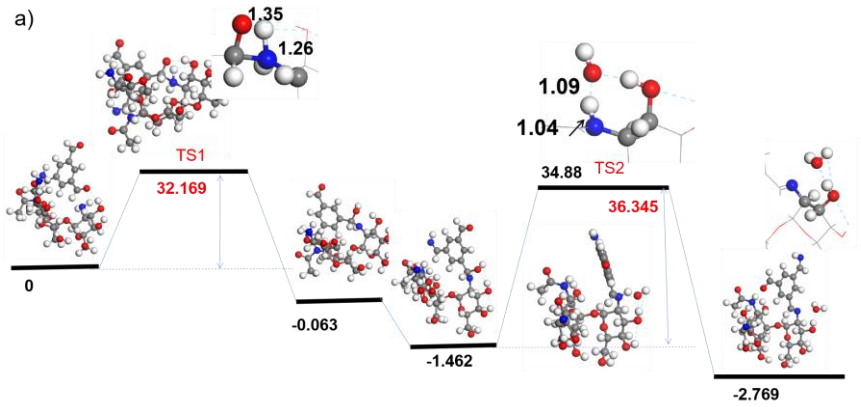
a)
1.35
1.26
TS1
32.169
0
-0.063
-1.462
1.09
1.04
34.88
TS2
36.345
-2.769

1

2

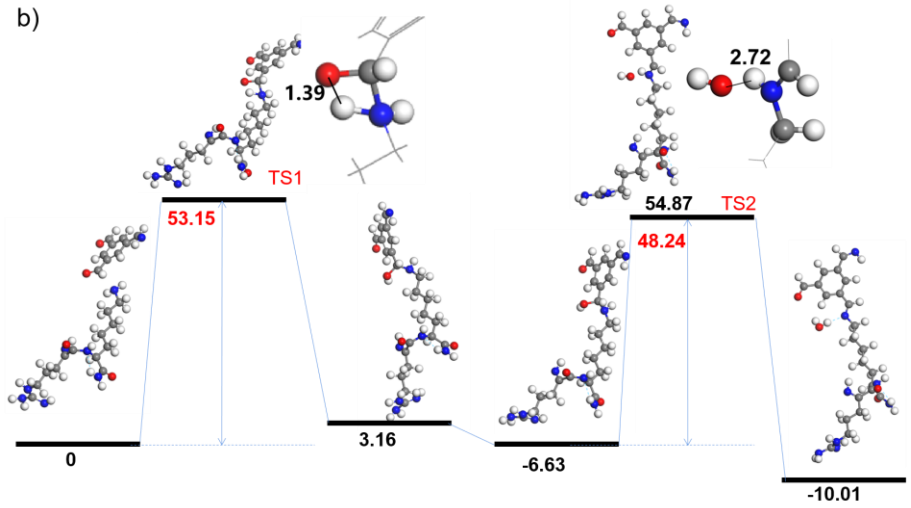
b)
1.39
TS1
53.15
0
3.16
2.72
54.87
TS2
48.24
-6.63
-10.01

3

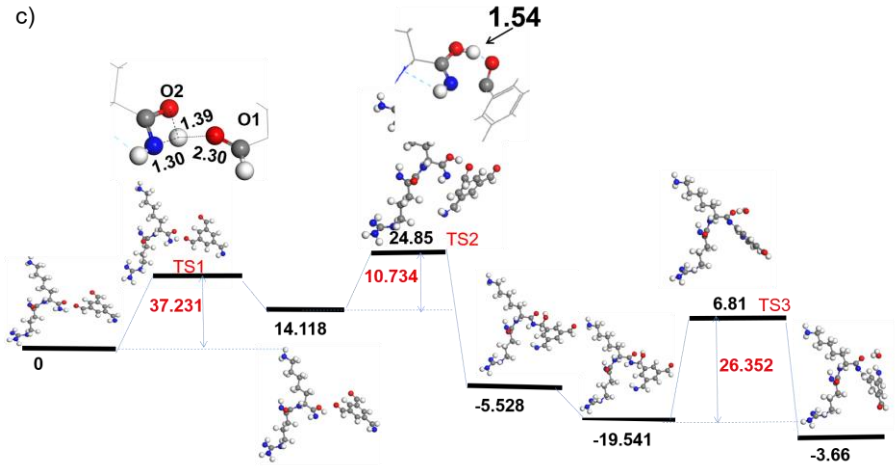
c)
1.54
O2
1.39
O1
1.30
2.30
TS1
37.231
0
14.118
24.85
TS2
10.734
-5.528
6.81
TS3
26.352
-19.541
-3.66

4

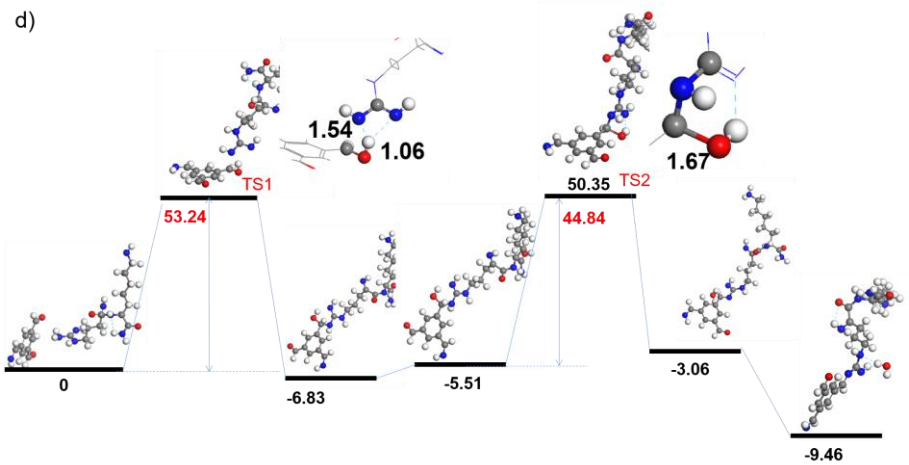

Fig. 8. Computation by density functional theory (DFT) to determine the lowest reaction pathways between : a) CMCS-l-Dy; b) TP5(1)-l-Dy (TP5 site 1); c) TP5(2)-l-Dy (TP5 site 2); and d) TP5(3)-l-Dy (TP5 site 3). The reaction energy and energy barrier are calculated by Eq. 5 and Eq. 6 in kcal/mol.

Density functional theory (DFT) was used to determine the reaction energy and energy barrier of imine linkages between TP5 and Dy (TP5-l-Dy, 'l' stands for linkage, similarly hereinafter) as well as those between CMCS and Dy (CMCS-l-Dy. The simplified models of CMCS, Dy and TP5 are shown in Fig. S7a-c. Only one reaction site is considered taking into account the repeatability of the amino groups in CMCS and the symmetry of Dy. The lowest energy pathway of the Schiff-base reaction between CMCS and Dy is shown in Fig. 8a. The first step of the reaction is the dehydrogenation from the amino group of Dy, which requires overcoming an energy barrier of 32.2 kcal/mol. The formation of CH-NH bond is thermodynamically favorable. This is followed by the cleavage of the oxhydryle group, which needs higher energy than the first step, reaching 36.3 kcal/mol. The formation and removing of H_2O molecule are thermodynamically favorable. Thus, the rate-limiting step of the reaction between CMCS and Dy is the cleavage of oxhydryle with an energy barrier of 36.3 kcal/mol.

There are three kinds of amino groups in TP5 which have different chemical environments (Fig. S7c). Thus, there are three -NH_2 sites that can be involved in the

Schiff-base reaction, which are marked as TP5(1)-l-Dy (Fig. 8b), TP5(2)-l-Dy (Fig. 8c) and TP5(3)-l-Dy (Fig. 8d), respectively. The Schiff-base reactions of TP5(1)-l-Dy and TP5(3)-l-Dy are similar. The rate-limiting step of both reactions is the dehydrogenation from the amino groups of TP5 (the first step), which needs to overcome an energy barrier of 53.15 and 53.24 kcal/mol, respectively. The reaction process to yield TP5(2)-l-Dy is more complex than those of the two other reactions. It begins with dehydrogenation from the amino group of TP5. But the H atom tends to bond with the adjacent oxygen atom (O2), and the process needs to overcome an energy barrier of 37.2 kcal/mol. In the second step, the hydrogen proton transfers from O2 to O1, which needs an energy of 10.7 kcal/mol. The formation of -C-NH bond is thermodynamically favorable. Subsequently, the cleavage of oxhydryle needs to overcome a barrier of 26.4 kcal/mol. Thus, the rate-limiting step of the reaction needs to overcome a barrier of 37.2 kcal/mol, which is only 0.9 kcal/mol higher than that of the Schiff-base reaction between CMCS and Dy. Thus, the -C=O group adjacent to the $-NH_2$ of TP5 could promote the Schiff-base reaction between TP5 and Dy to form TP5(2)-l-Dy. Moreover, the two other $-NH_2$ sites of TP5 may also participate in the Schiff-base reaction in spite of higher energy barrier. Hence, although the energy barrier of TP5-l-Dy is higher than that of CMCS-l-Dy, both reactions proceed concomitantly in a competitive way.

Furthermore, it is worth noting that the gelation time of blank hydrogel without TP5 is shorter than that of hydrogel containing TP5 (data not shown). Therefore, the presence of TP5 affects the crosslinking between CMCS and Dy because TP5 reacts competitively with Dy and formation of TP5-l-Dy does not contribute to the crosslinking due to steric effect. When TP5 is mixed with Dy, it can theoretically and experimentally react with Dy via Schiff base reaction, which is in full agreement with the results obtained by FT-IR (Fig. 1), NMR (Fig. 2), and SEM (Fig. S4), and TP5 release (Fig. 6 and 7).

4. Conclusion

This work focused on the synthesis and characterization of a novel drug delivery system based on dynamic hydrogels for the sustainable release of an immunostimulant – thymopentin (TP5). The hydrogels were prepared via *in situ* gelation of O-carboxymethyl chitosan with a dynamer made from Jefamine and BTA in aqueous solution by imine bonding, in the presence or absence of TP5. These hydrogels display a porous structure, outstanding rheological properties and excellent pH-sensitive swelling performance. Analyses showed that TP5 is partly attached to the hydrogel network by imine bonding, together with free TP5 molecules adsorbed by physical forces into the hydrogel pore walls. *In vitro* release showed a burst release in the first 24 h, followed by a slower release to reach a plateau up to 168 h. The maximum release rate depends on various factors such as drug content, drug loading and release conditions. Data show that only free TP5 is released under in vitro conditions. Covalently attached TP5 is not released due to the stability of imine bonds at pH 7.4. Density functional theory study allowed to better understand the chemical combination between the hydrogel's components and the drug. All these findings suggest that *in situ* gelation of water soluble CMCS with a 3D dynamer is a means of choice to design efficient release systems of hydrophilic drugs, in particular those containing amino groups which can be covalently attached to the hydrogel network. Last but not least, this study offers a simple and environmentally friendly strategy to prepare bioactive and biodegradable hydrogels for drug delivery systems.

Acknowledgement

This work is supported by the scholarship from China Scholarship Council (CSC), and the Institut Européen des Membranes (Exploratory project "Biostent - Health" of the Internal IEM Call 2017).

References

[1] G. Goldstein, T.K. Audhya, Thymopoietin to thymopentin: experimental studies, Surv. Immunol. Res., 4 (1985) 1, https://doi.org/10.1007/BF02919050.

[2] D.H. Schlesinger, G. Goldstein, The amino acid sequence of thymopoietin II, Cell, 5 (1975) 361-365, https://doi.org/10.1016/0092-8674(75)90054-9.
[3] G. Goldstein, M.P. Scheid, E.A. Boyse, D.H. Schlesinger, J. Van Wauwe, A synthetic pentapeptide with biological activity characteristic of the thymic hormone thymopoietin, Science, 204 (1979) 1309-1310, https://doi.org/10.1126/science.451537.
[4] S. Lin, B. Cai, G. Quan, T. Peng, G. Yao, C. Zhu, Q. Wu, H. Ran, X. Pan, C. Wu, Novel strategy for immunomodulation: Dissolving microneedle array encapsulating thymopentin fabricated by modified two-step molding technology, Eur. J. Pharm. Biopharm., 122 (2018) 104-112, https://doi.org/10.1016/j.ejpb.2017.10.011.
[5] T. Zhang, X. Qin, X. Cao, W. Li, T. Gong, Z. Zhang, Thymopentin-loaded phospholipid-based phase separation gel with long-lasting immunomodulatory effects: in vitro and in vivo studies, Acta Pharmacologica Sinica, 40 (2019) 514-521, https://doi.org/10.1038/s41401-018-0085-8.
[6] B. Bodey, B. Bodey Jr, S.E. Siegel, H.E. Kaiser, Review of thymic hormones in cancer diagnosis and treatment, Int. J. Immunopharmacol, 22 (2000) 261-273, https://doi.org/10.1016/S0192-0561(99)00084-3.
[7] B. Kantharia, N. Goulding, N. Hall, J. Davies, P. Maddison, P. Bacon, M. Farr, J. Wojtulewski, K. Englehart, S. Liyanage, Thymopentin (TP-5) in the treatment of rheumatoid arthritis, Rheumatology, 28 (1989) 118-123, https://doi.org/10.1093/rheumatology/28.2.118.
[8] Y. Wang, X. Ke, J.S. Khara, P. Bahety, S. Liu, S.V. Seow, Y. Yang, P.L.R. Ee, Synthetic modifications of the immunomodulating peptide thymopentin to confer anti-mycobacterial activity, Biomaterials, 35 (2014) 3102-3109, https://doi.org/10.1016/j.biomaterials.2013.12.049.
[9] X. Cao, Y. Li, Y. Guo, F. Cao, Thymopentin improves cardiac function in older patients with chronic heart failure, Anatolian journal of cardiology, 17 (2017) 24, https://doi.org/10.14744/AnatolJCardiol.2016.6692.
[10] R. Colle, T. Ceschia, A. Colatutto, F. Biffoni, Use of thymopentin in autoimmune hemolytic anemia due to chronic lymphocytic leukemia, Current therapeutic research, 44 (1988) 1045-1049.
[11] M. Zhu, W. Wan, H. Li, J. Wang, G. Chen, X. Ke, Thymopentin enhances the generation of T-cell lineage derived from human embryonic stem cells in vitro, Exp. Cell Res., 331 (2015) 387-398, https://doi.org/10.1016/j.yexcr.2014.12.012.
[12] M.S. Kondratyev, S.M. Lunin, A.V. Kabanov, A.A. Samchenko, V.M. Komarov, E.E. Fesenko, E.G. Novoselova, Structural and dynamic properties of thymopoietin mimetics, J. Biomol. Struct. Dyn., 32 (2014) 1793-1801, https://doi.org/10.1080/07391102.2013.834851.
[13] Y. Wang, Y. Cao, Y. Meng, Z. You, X. Liu, Z. Liu, The novel role of thymopentin in induction of maturation of bone marrow dendritic cells (BMDCs), Int. Immunopharmacol., 21 (2014) 255-260, https://doi.org/10.1016/j.intimp.2014.05.011.
[14] J.P. Tischio, J.E. Patrick, H.S. Weintraub, M. Chasin, G. Goldstein, Short in vitro half- life of thymopoietin 32–36 pentapeptide in human plasma, Int. J. Pept. Protein

Res., 14 (1979) 479-484, https://doi.org/10.1111/j.1399-3011.1979.tb01959.x.
[15] T. Audhya, G. Goldstein, Thymopentin (TP- 5) potency in vivo is enhanced by slow infusion, International journal of peptide protein research, 22 (1983) 568-572, https://doi.org/10.1111/j.1399-3011.1983.tb02130.x.
[16] X. Jin, Y. Xu, J. Shen, Q. Ping, Z. Su, W. You, Chitosan-glutathione conjugate-coated poly (butyl cyanoacrylate) nanoparticles: promising carriers for oral thymopentin delivery, Carbohydr. Polym., 86 (2011) 51-57, https://doi.org/10.1016/j.carbpol.2011.03.050.
[17] Y. Xu, G. Li, W. Zhuang, H. Yu, Y. Hu, Y. Wang, Micelles prepared from poly (N-isopropylacrylamide-co-tetraphenylethene acrylate)-b-poly [oligo (ethylene glycol) methacrylate] double hydrophilic block copolymer as hydrophilic drug carrier, Journal of Materials Chemistry B, 6 (2018) 7495-7502, https://doi.org/10.1039/C8TB02247J.
[18] J. Zuo, T. Gong, X. Sun, Y. Huang, Q. Peng, Z. Zhang, Multivesicular liposomes for the sustained release of thymopentin: stability, pharmacokinetics and pharmacodynamics, Die Pharmazie-An International Journal of Pharmaceutical Sciences, 67 (2012) 507-512, https://doi.org/10.1691/ph.2012.1126.
[19] Y. Zhang, X. Wu, Y. Han, F. Mo, Y. Duan, S. Li, Novel thymopentin release systems prepared from bioresorbable PLA–PEG–PLA hydrogels, Int. J. Pharm., 386 (2010) 15-22, https://doi.org/10.1016/j.ijpharm.2009.10.045.
[20] Y. Hu, Y. Liu, X. Qi, P. Liu, Z. Fan, S. Li, Novel bioresorbable hydrogels prepared from chitosan- graft- polylactide copolymers, Polym. Int., 61 (2012) 74-81, https://doi.org/10.1002/pi.3150.
[21] Y. Yin, D. Chen, M. Qiao, Z. Lu, H. Hu, Preparation and evaluation of lectin-conjugated PLGA nanoparticles for oral delivery of thymopentin, J. Controlled Release, 116 (2006) 337-345, https://doi.org/10.1016/j.jconrel.2006.09.015.
[22] J. Li, D. Mooney, Designing hydrogels for controlled drug delivery, Nature Reviews Materials, 1 (2016) 1-17, https://doi.org/10.1038/natrevmats.2016.71.
[23] J. Zhao, X. Zhao, B. Guo, P.X. Ma, Multifunctional interpenetrating polymer network hydrogels based on methacrylated alginate for the delivery of small molecule drugs and sustained release of protein, Biomacromolecules, 15 (2014) 3246-3252, https://doi.org/10.1021/bm5006257.
[24] S. Peers, A. Montembault, C. Ladavière, Chitosan hydrogels for sustained drug delivery, J. Controlled Release, 326 (2020) 150-163, https://doi.org/10.1016/j.jconrel.2020.06.012.
[25] X. Yang, G. Liu, L. Peng, J. Guo, L. Tao, J. Yuan, C. Chang, Y. Wei, L. Zhang, Highly efficient self- healable and dual responsive cellulose- based hydrogels for controlled release and 3D cell culture, Adv. Funct. Mater., 27 (2017) 1703174, https://doi.org/10.1002/adfm.201703174.
[26] J. Su, B. Hu, W.L. Lowe Jr, D.B. Kaufman, P.B. Messersmith, Anti-inflammatory peptide-functionalized hydrogels for insulin-secreting cell encapsulation, Biomaterials, 31 (2010) 308-314, https://doi.org/10.1016/j.biomaterials.2009.09.045.
[27] J.M. Reichert, Trends in development and approval times for new therapeutics in

the United States, Nature Reviews Drug Discovery, 2 (2003) 695-702, https://doi.org/10.1038/nrd1178.
[28] F. Su, J. Wang, S. Zhu, S. Liu, X. Yu, S. Li, Synthesis and characterization of novel carboxymethyl chitosan grafted polylactide hydrogels for controlled drug delivery, Polym. Adv. Technol., 26 (2015) 924-931, https://doi.org/10.1002/pat.3503.
[29] S.T.K. Raja, T. Prakash, A. Gnanamani, Redox responsive albumin autogenic nanoparticles for the delivery of cancer drugs, Colloids Surf. B. Biointerfaces, 152 (2017) 393-405, https://doi.org/10.1016/j.colsurfb.2017.01.044.
[30] Y. Lin, H. Liang, C. Chung, M. Chen, H. Sung, Physically crosslinked alginate/N, O-carboxymethyl chitosan hydrogels with calcium for oral delivery of protein drugs, Biomaterials, 26 (2005) 2105-2113, https://doi.org/10.1016/j.biomaterials.2004.06.011.
[31] A. Lu, E. Petit, S. Li, Y. Wang, F. Su, S. Monge, Novel thermo-responsive micelles prepared from amphiphilic hydroxypropyl methyl cellulose-block-JEFFAMINE copolymers, Int. J. Biol. Macromol., 135 (2019) 38-45, https://doi.org/10.1016/j.ijbiomac.2019.05.087.
[32] Y. Zhang, C. Pham, R. Yu, E. Petit, S. Li, M. Barboiu, Dynamic hydrogels based on double imine connections and application for delivery of fluorouracil, Frontiers in Chemistry, 8 (2020) 739, https://doi.org/10.3389/fchem.2020.00739.
[33] R. Yu, Y. Zhang, M. Barboiu, M. Maumus, D. Noël, C. Jorgensen, S. Li, Biobased pH-responsive and self-healing hydrogels prepared from *O*-carboxymethyl chitosan and a 3-dimensional dynamer as cartilage engineering scaffold, Carbohydr. Polym., 244 (2020) 116471, https://doi.org/10.1016/j.carbpol.2020.116471.
[34] R. Yu, L. Cornette de Saint-Cyr, L. Soussan, M. Barboiu, S. Li, Anti-bacterial dynamic hydrogels prepared from O-carboxymethyl chitosan by dual imine bond crosslinking for biomedical applications, Int. J. Biol. Macromol., 167 (2020) 1146-1155, https://doi.org/10.1016/j.ijbiomac.2020.11.068.
[35] S. Sharma, P. Jain, S. Tiwari, Dynamic imine bond based chitosan smart hydrogel with magnified mechanical strength for controlled drug delivery, Int. J. Biol. Macromol., 160 (2020) 489-495, https://doi.org/10.1016/j.ijbiomac.2020.05.221.
[36] T. Sun, D. Zhou, F. Mao, Y. Zhu, Preparation of low-molecular-weight carboxymethyl chitosan and their superoxide anion scavenging activity, Eur. Polym. J., 43 (2007) 652-656, https://doi.org/10.1016/j.eurpolymj.2006.11.014.
[37] S. Dash, P.N. Murthy, L. Nath, P. Chowdhury, Kinetic modeling on drug release from controlled drug delivery systems, Acta Pol. Pharm., 67 (2010) 217-223.
[38] A.M. Craciun, L.M. Tartau, M. Pinteala, L. Marin, Nitrosalicyl-imine-chitosan hydrogels based drug delivery systems for long term sustained release in local therapy, Journal of Colloid and Interface Science, 536 (2019) 196-207, https://doi.org/10.1016/j.jcis.2018.10.048.
[39] B. Delley, From molecules to solids with the DMol 3 approach, The Journal of chemical physics, 113 (2000) 7756-7764, https://doi.org/10.1063/1.1316015.
[40] S. Grimme, J. Antony, S. Ehrlich, H. Krieg, A consistent and accurate ab initio parametrization of density functional dispersion correction (DFT-D) for the 94 elements

H-Pu, The Journal of chemical physics, 132 (2010) 154104, https://doi.org/10.1063/1.3382344.
[41] A. Klamt, G. Schüürmann, COSMO: a new approach to dielectric screening in solvents with explicit expressions for the screening energy and its gradient, Journal of the Chemical Society, Perkin Transactions 2, (1993) 799-805, https://doi.org/10.1039/P29930000799.
[42] N. Govind, M. Petersen, G. Fitzgerald, D. King-Smith, J. Andzelm, A generalized synchronous transit method for transition state location, Computational materials science, 28 (2003) 250-258, https://doi.org/10.1016/S0927-0256(03)00111-3.
[43] H.R. Rizvi, M.J. Khattak, A.A. Gallo, Rheological and mechanistic characteristics of Bone Glue modified asphalt binders, Construction Building Materials, 88 (2015) 64-73, https://doi.org/10.1016/j.conbuildmat.2015.03.023.
[44] R. Singh, K. Rao, A. Anjaneyulu, G. Patil, Moisture sorption properties of smoked chicken sausages from spent hen meat, Food Res. Int., 34 (2001) 143-148, https://doi.org/10.1016/S0963-9969(00)00145-9.
[45] P. Xue, N. Sun, Y. Li, S. Cheng, S. Lin, Targeted regulation of hygroscopicity of soybean antioxidant pentapeptide powder by zinc ions binding to the moisture absorption sites, Food Chem., 242 (2018) 83-90, https://doi.org/10.1016/j.foodchem.2017.09.025.
[46] J.B. Vaughn Jr, R.L. Stephens, R.E. Lenkinski, N.R. Krishna, G.A. Heavner, G. Goldstein, Proton NMR investigation of Ln3+ complexes of thymopoietin32–36, Biochimica et Biophysica Acta (BBA) - Protein Structure, 671 (1981) 50-60, https://doi.org/10.1016/0005-2795(81)90093-3.
[47] S. Li, A. El Ghzaoui, E. Dewinck, Rheology and drug release properties of bioresorbable hydrogels prepared from polylactide/poly (ethylene glycol) block copolymers, in: Macromol. Symp., Wiley Online Library, 2005, pp. 23-36, https://doi.org/10.1002/masy.200550403.
[48] N. Bhattarai, J. Gunn, M. Zhang, Chitosan-based hydrogels for controlled, localized drug delivery, Adv. Drug Del. Rev., 62 (2010) 83-99, https://doi.org/10.1016/j.addr.2009.07.019.
[49] S.V. Madihally, H.W. Matthew, Porous chitosan scaffolds for tissue engineering, Biomaterials, 20 (1999) 1133-1142, https://doi.org/10.1016/S0142-9612(99)00011-3.
[50] Y. Liang, X. Zhao, T. Hu, Y. Han, B. Guo, Mussel-inspired, antibacterial, conductive, antioxidant, injectable composite hydrogel wound dressing to promote the regeneration of infected skin, Journal of colloid interface science, 556 (2019) 514-528, https://doi.org/10.1016/j.jcis.2019.08.083.
[51] X. Lv, W. Zhang, Y. Liu, Y. Zhao, J. Zhang, M. Hou, Hygroscopicity modulation of hydrogels based on carboxymethyl chitosan/Alginate polyelectrolyte complexes and its application as pH-sensitive delivery system, Carbohydr. Polym., 198 (2018) 86-93, https://doi.org/10.1016/j.carbpol.2018.06.058.
[52] P. Gupta, K. Vermani, S. Garg, Hydrogels: from controlled release to pH-responsive drug delivery, Drug Discovery Today, 7 (2002) 569-579,

https://doi.org/10.1016/S1359-6446(02)02255-9.
[53] M.G. Bernengo, A. Appino, M. Bertero, M. Novelli, M.T. Fierro, G.C. Doveil, F. Lisa, Thymopentin in Sezary syndrome, JNCI: Journal of the National Cancer Institute, 84 (1992) 1341-1346, https://doi.org/10.1093/jnci/84.17.1341.
[54] A. Patruno, P. Tosco, E. Borretto, S. Franceschelli, P. Amerio, M. Pesce, S. Guglielmo, P. Campiglia, M.G. Bernengo, R. Fruttero, Thymopentin down-regulates both activity and expression of iNOS in blood cells of Sézary syndrome patients, Nitric Oxide, 27 (2012) 143-149, https://doi.org/10.1016/j.niox.2012.06.002.
[55] S. Zhao, M.M. Abu-Omar, Recyclable and malleable epoxy thermoset bearing aromatic imine bonds, Macromolecules, 51 (2018) 9816-9824, https://doi.org/10.1021/acs.macromol.8b01976.
[56] J. Siepmann, N.A. Peppas, Higuchi equation: derivation, applications, use and misuse, Int. J. Pharm., 418 (2011) 6-12, https://doi.org/10.1016/j.ijpharm.2011.03.051.